https://ntrs.nasa.gov/search.jsp?R=19950004591 2020-06-16T11:33:54+00:00Z

NASA
Technical
Paper
3482

1994

Subjective Evaluations of Integer Cosine Transform Compressed Galileo Solid State Imagery

Richard F. Haines and Yaron Gold,
RECOM Technologies, Inc., Moffett Field, California
Terry Grant and Sherry Chuang
Ames Research Center, Moffett Field, California

National Aeronautics and
Space Administration

Ames Research Center
Moffett Field, California 94035-1000

SUBJECTIVE EVALUATIONS OF INTEGER COSINE TRANSFORM COMPRESSED GALILEO SOLID STATE IMAGERY

Richard F. Haines,* Yaron Gold,* Terry Grant, and Sherry L. Chuang
Ames Research Center

SUMMARY

This paper describes a study conducted for the Jet Propulsion Laboratory (JPL), Pasadena, California, using 15 volunteer evaluators from 12 institutions involved in the Galileo Solid State Imaging (SSI) experiment (ref. 1). The objective of the study was to determine the impact of integer cosine transform (ICT) compression (ref. 2) using specially formulated quantization (q) tables and compression ratios on acceptability of the resulting 800 × 800 × 8 monochromatic astronomical images as evaluated visually by Galileo SSI mission scientists. Fourteen different images in seven image groups were evaluated. Each evaluator viewed two versions of the same image side by side on a high-resolution monitor; each was compressed using a different q level. First the evaluators selected the image with the highest overall quality to support them in their visual evaluations of image content. Next they rated each image using a scale from one to five indicating its judged degree of usefulness. Up to four preselected types of images with and without noise were presented to each evaluator based on results of a previously administered survey of their image preferences. Data are presented that show: (1) Radiation noise reduces the acceptable ICT compression ratio, particularly when high spatial frequency information is present. In the most extreme case, compression of the same image was reduced by 19 times, from 57:1 to <3:1, due to noise. (2) The highest ICT compression achieved was about 85 for a relatively homogeneous dark surface image with multiple small lightning phenomena visible. The next highest ICT compression (from 51 to 72) was associated with an image of a gaseous surface (Jupiter) without limb. (3) Of the 4 q tables studied, number 2 yielded the greatest acceptable ICT compression in 8 of the 14 images studied. (4) It was not possible to predict a priori what maximum ICT compression (using the q tables) would be attainable for these kinds of images. Visual ratings made by experienced evaluators are needed for each type of image to determine the impact of particular q tables and q levels on maximum acceptable ICT compression.

*RECOM Technologies, Inc.

INTRODUCTION

The Galileo spacecraft was launched in October 1989 and will reach Jupiter and its moons in late 1995. Its mission is varied, including an Io flyby, releasing a probe into the Jovian atmosphere (with probe data capture and transmission to earth), Jupiter orbital insertion, and 10 satellite encounters with Ganymede, Callisto, and Europa. In April 1991 a command was sent to the spacecraft to open its 1.8m X-band high-gain antenna (HGA), but it failed to deploy. Unless it can be made to operate, all communications between Earth and the spacecraft will be through one of the two S-band low-gain antennas (LGA) which, at Jupiter's range, can support a telemetry data rate of only 10 bits/sec (compared to 134 kbits/sec in the HGA mode).

A contingency plan known as the "Galileo S-Band Contingency Mission" was devised to cope with the use of the LGA. The plan includes major ground upgrades and inflight reprogramming of the spacecraft's microprocessors to perform advanced signal processing of sensor data to help boost the effective data rate. These onboard algorithms include advanced error-correction coding, "packetizing," and data compression schemes. A lossy image compression scheme (ICT) was proposed (refs. 2 and 3); it is computationally simple enough for spacecraft implementation. And so why was this study needed?

Digital imagery received from the Galileo spacecraft will be manipulated and studied in many different ways. One general class of manipulations is photometric, where the intensity of every picture element (pixel) must be accurately transmitted, recorded, and processed. Visual assessments may or may not be made. A second general class, however, involves examining the image visually to locate and identify features of interest and qualitatively evaluate them. Such examinations may precede or follow some kinds of image manipulations such as simple luminance stretching, contrast enhancement, and feature identification. The present study was deliberately designed, at the request of JPL, to address the second type of image manipulations since it is not known whether important features in an image from the Galileo SSI experiment will be lost or distorted due to the ICT quantization process. Preliminary work by Ekroot (ref. 4) using the ICT

algorithm on Galileo images has shown that the compression ratio and consequent distortion cannot be easily predicted before compression without considering various information about each image. Her findings and preliminary interviews with SSI team members led to the inclusion of a number of different image classes in the present study.

The image compression algorithm planned for use during the Galileo S-band mission is an 8×8 multiplication free ICT approach. It may be considered as an integer approximation of the popular discrete cosine transform (DCT) scheme (ref. 5). While the ICT (described in appendix A) is much easier to implement than the DCT, it yields comparable performance (ref. 3).

It is well known that image compression techniques may or may not produce visually perceptible losses or unacceptable distortions of useful features within a digital image. If so-called lossy compression techniques are employed, will image features be altered in any significant way and, more importantly, will such alterations be perceptible to the scientists who must work with these images? Indeed, there are no universally acceptable objective standards for evaluating the effects of image compression. As Haskell and Steele (ref. 6) state, "Only when perception is properly understood will we have accurate objective measures. However, the day when we can, with confidence, objectively evaluate a new impairment without recourse to subjective testing seems very remote." Nevertheless, experimental psychological and human factors techniques are available to relate the acceptability of visual features of an image with different types and levels of image compression. Such subjectively determined techniques were used here.

This experimental, psychophysical study was conducted to assess the quality of images that result from the application of the ICT algorithm (appendix A) and sets of specially developed q tables (appendix B) used to compress and decompress images representative of the Galileo SSI experiment. The primary question addressed here was: What is the acceptable image compression ratio (or range of ratios) using different q tables in the ICT algorithm?

METHODOLOGY

Basic Experimental Assumptions and Approach

We assumed that images could be grouped according to their visually based scientific features of interest and that experienced investigators with similar interests in these images would have common requirements for acceptable visual fidelity. Application of these assumptions made it possible to design an experiment which involved a reasonably small number of generally representative images and interested members of the Galileo SSI science team.

The following general activities were carried out and are discussed in detail in following sections: (1) Informal meetings were held with several members of the 12-member SSI team. From these meetings a classification of images and a greater understanding of how different classes of images are studied resulted. (2) A pretest survey was developed and sent to the SSI personnel. (3) An experimental design and approach was developed that permitted valid statistical comparisons of the variables of interest. The data collection approach was planned so that judgment variability within individual evaluator's data would be distributed randomly across the administration of the other variables to not unduly bias any particular test condition. (4) Hardware and software were configured to support data collection. Three independent computer workstations were used to simultaneously present the imagery to three separate groups of evaluators. (5) Subjective judgments and ratings were made by scientists participating in a Galileo SSI Compression Workshop held at Ames Research Center on July 22, 1993. (6) The experimental results were preliminarily analyzed and presented at the workshop. This report presents the completed statistical analysis of all data.

Identification of basic imagery classes– The SSI team members indicated several imagery classes were of interest to them. The images presented were selected from seven classes out of a larger set of image data files provided by JPL (table 1). There were also various images with superimposed noise (table 2).

Table 1. Image classes studied

Solid surface with limb
Solid surface without limb
Solid surface with terminator
Gaseous surface without limb
Small bodies (e.g., asteroid)
Dark side phenomena/lightning
Rings

Table 2. Image details

Image class name	Body	File name	Noise	Magnification	q tables studied		
					1	2	3
Solid with limb	Europa	r.6.r		×2	0	1	2
	Europa	r6.noise.r	×	×2	0	1	2
	Io	r.9.r		×2	0	1	2
Solid, no limb	Ganymede	r.4.r		×2	0	1	2
	Ganymede	rq538.g.r	×	×2	0	1	2
	Io	sr7.raw.r		×2	0	1	2
	Io	sr7.noise.r	×	×2	0	1	2
Solid with terminator	Callisto	r.1.r		×2	0	1	2
Gaseous, no limb	Jupiter	r.14.r		×1	0	2	3
	Jupiter	r.15.r		×1	0	2	3
	Jupiter	rq538.j4o.r	×	×1	0	2	3
Small bodies	Gaspra	rq538.gas.r		×2	0	1	2
Dark side/lightning	Earth	rq538.litn.r		×2	0	1	2
Rings	Saturn	r.11.r		×2	0	1	2

Pretest survey– A survey (appendix C) was sent to 40 SSI team members and related staff (site managers, interdisciplinary scientists (IDS), and associates) representing 10 institutions and NASA participants to determine what kinds of imagery and scientific features they worked with, how they planned to use the Galileo imagery, and what preprocessing requirements they had. Thirteen of the 40 SSI team members (representing 12 institutions) completed the survey before the Ames workshop. Telephone calls were made to the SSI members who did not complete the questionnaire. The survey responses permitted us to match volunteer test subjects at the workshop with classes of test images of most interest to them.

A special line drawing was included with the survey (appendix C) to explain the differences between spatial versus gray-scale resolution in ICT compression. There were three possible resolution variants: (1) no compression, (2) low gray-scale resolution/high spatial resolution, and (3) high gray-scale resolution/low spatial resolution. The drawing helped the team members more accurately respond to the survey. In addition, seven black and white examples of the various image classes were included. The survey results are presented in appendix D.

Three topics are considered in the survey: (1) type of information extraction used, (2) types of image preprocessing used, and (3) relevanced and spatial versus gray-scale resolution requirements.

Type of information extraction used: Of the 17 responses obtained, 1 respondent was only interested in visual information extraction and listed 5 of the image classes as being of interest and 4 kinds of applications (morphological shapes/structures, horizontal distance measurement, region boundaries, and depth from stereopsis). Fourteen respondents indicated a broad interest in applying both visual information extraction and photometric operations. One of them was interested in only one type of image while another said he would study all seven of the image categories provided on the survey. Most respondents marked four or five image categories. As expected, a wide variety of visual information extraction approaches and photometric operations were marked. The results tended to confirm what several workshop participants stated—namely, while the respondents may rely primarily on visual information extraction approaches in

their work, they may also perform various image enhancement operations (in the photometric measurement domain) to better see details. One respondent was interested only in performing photometric operations on images and marked all seven of the image classes as being of interest as well as instrument calibration.

Types of image preprocessing used: This survey question was included to gain a better idea of how images are preprocessed. Every respondent marked two or more items (highest frequency items included noise reduction, contrast enhancement, and artifact removal); 10 respondents marked 5 or more items. "Other" items that were handwritten in the space provided on the survey included radiometric calibration, item classification, clustering analysis, motion analysis, sun angle correction, pseudocoloring, histogram equalization, nonlinear transforms, and low pass filtering.

Relevance and spatial versus gray-scale resolution requirements: (1) Relevance of various ways to extract information. The survey included boxes to mark the relevance of each of the visual information extraction approaches used and the relevance of the photometric operations conducted by each respondent. In addition, a matrix of boxes permitted the respondents to indicate their relative trade-off of importance for each visual information extraction approach and photometric operation along a spatial (high-detail) to gray-scale (intensity) axis. Almost all respondents indicated that determining morphological shapes/structures had the greatest relevance to them (only 3 ranked it under 10). Determining the horizontal distance of details was ranked as the second most used approach in the visual domain, and the remaining items were ranked in no particular order. Clearly, the respondents relied on a wide and creative variety of techniques for studying astronomical imagery. Of the three items listed on the survey, two were cited most often as being the most relevant photometric operations (reflectance measurements and multispectral ratios) with the shape from shading cited in third place or not at all by other respondents.

(2) Spatial versus gray scale resolution requirements. As expected, there was a high correspondence indicated between spatial-resolution/visual-information-extraction items and gray-scale resolution/photometric-operations items. Interestingly, one visual information extraction approach ("region boundaries") was marked by several respondents as involving a high-gray-scale resolution preference. This suggests that visual contrast optimization between adjacent surface details is considered an effective means of identifying the presence (and identity?) of different kinds of surface regions. Two other types of images that elicited a high-gray-scale preference were "plume studies on limbs" and "brightness gradient analysis."

The pre-workshop survey provided valuable insights about the types of images the SSI team members and others actually work on and provided information about how they manipulate the images. The findings were used to structure the experimental design.

Experimental design and approach– The experimental design used to administer the variables of interest can be characterized as a $4 \times 32 \times 2 \times 15$ parametric design (fig. 1). The test variables are given in table 3.

		q table and quantization levels (row y)											
		q table 0			q table 1			q table 2			q table 3		
y ►		1	2	3	1	2	3	1	2	3	1	2	3
Image 1	Noise												
	No noise												
Image 2	Noise												
	No noise												

Figure 1. Experimental design.

Table 3. Test variables

Factor	No.	Comments
Quantization levels	3	From 2 to 72
q table	4	Each evaluator was presented only 3; see appendix B for details
Image type	2	No noise; with noise
Evaluators	15	

The presentation order of the test conditions (fig. 1) was horizontal—the three quantization/compression level conditions were completed for q table 0 before proceeding to the next three cells within q tables 1–3. Each evaluator rated three q tables on each image. The remaining two tables were presented in random order. Evaluators were first presented the no noise image, then its

corresponding noise image version was presented when one was available. Because each group of three evaluators was presented a different set of images, this factor does not constitute an experimental variable—from a statistical point of view, each image type is considered to be a separate experiment. While they are not absolutely independent from each other, the results found for one image type should not be compared with the results for another image type.

Approach– Written test instructions (appendix E) were given to all evaluators prior to testing and were also read out loud to them just before data collection started. Two separate judgments were made for every pair of images: (1) select the image that had the highest overall quality to support the evaluator in their work, and (2) rate both images using a numeric scale from 1 to 5, where 1 = totally useless, 3 = about average usefulness/value/merit, and 5 = highest possible usefulness/value/merit. During data collection it was stated that a score of 3 represented average or nominal image acceptance while a score of 2 represented a relatively poor image that probably would not be very useful.

Ideally, three or more evaluators in a given image type group were asked to rate image quality; each succeeding evaluator was presented with a progressively smaller range of q levels. This progressive division method is illustrated in figure 2. For example, the first evaluator was presented 1 of the 2 side-by-side images at q = 2 (level 1 in fig. 2), or at q = 36 (level 3 in fig. 2).

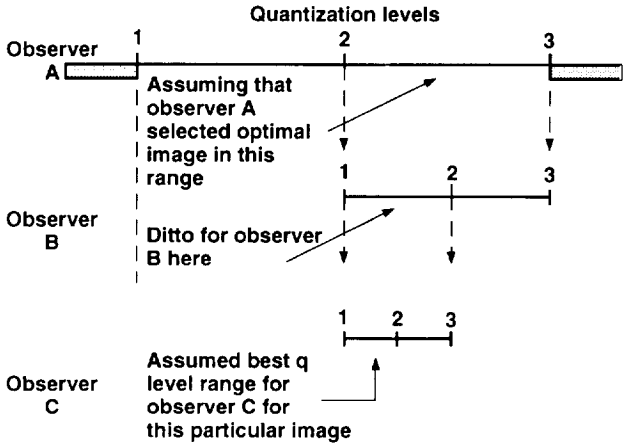

Figure 2. Method of Progressive Division.

After observer A made subjective ratings of each image, the second pair of the same images was displayed. One was again set at q = 2 and the other was set at q = 18 (half of the previous full range shown by q = 2 in fig. 2). After the second pair of images was visually rated the third pair of images was displayed with one image set at q = 18 and the other set at q = 36 (the second half of the previous full range). The evaluator was not told anything about the q levels employed or which side (left or right) each image was on (the images were randomly positioned). For purposes of most evaluators rating the methodology, let us assume the observer selected the best image to lie somewhere between q = 2 and q = 3.

The objective was to identify the quantization levels that separated an unacceptable from an acceptable rating. A rating of 3 was considered the threshold between an acceptable and an unacceptable image. Thus, images given a score larger or smaller than three were used to determine when to decrease or increase the quantization levels, respectively, in subsequent testing.

Images studied: Table 2 provides a brief description of the 14 images tested. All images except r.14.r, r.15.r, and rq538j4o.r were enlarged times 2 for display. All but sr7.raw.r and sr7.noise.r were 800 × 800 pixel formats. The three images of Jupiter were presented without zoom. All images were cropped to (a) fit two images side by side on the monitor for simultaneous comparison, (b) permit the images to be enlarged, and (c) reduce the amount of dark "space" background surrounding them. Care was taken to avoid cropping important features. In addition, most of the images were enlarged to better display the visual effects of the ICT compression on various image details. Actual Voyager data and simulated Galileo data file parameters are given in appendix F.

Noise images: Four images contained superimposed noise that would influence the image appearance after compression. Three types of simulated radiation noise were studied (figs. 3–5). Two (types B and D) consisted of random dots and short lines at random positions and orientations. Noise type C consisted of identical pairs of dots and short inclined lines separated by about one-twentieth of the frame dimension.

Hardware and software configuration–SUN SparcStations with 21-in. color monitors were used. The front panel of the three independent SUN color monitors were preset to full brightness, mid-range (detent) contrast and mid-range (detent) vertical slew. Individual red, green, and blue pixel diameters and pixel-to-pixel distances were measured with a 60 power microscopic enlargement and linear calibration scale. Appendix G presents these dimensions. The variations in pixel dimensions for the three monitors was considered to be insignificant because the displayed imagery pixels were scaled to be displayed in groups of four pixels (blank, red, green, and blue), which were well below the limit of the evaluators' visual resolution (acuity). All evaluators sat with their eyes approximately 18–24 in. from the monitor to ensure that four-pixel groups could not be perceived with clarity.

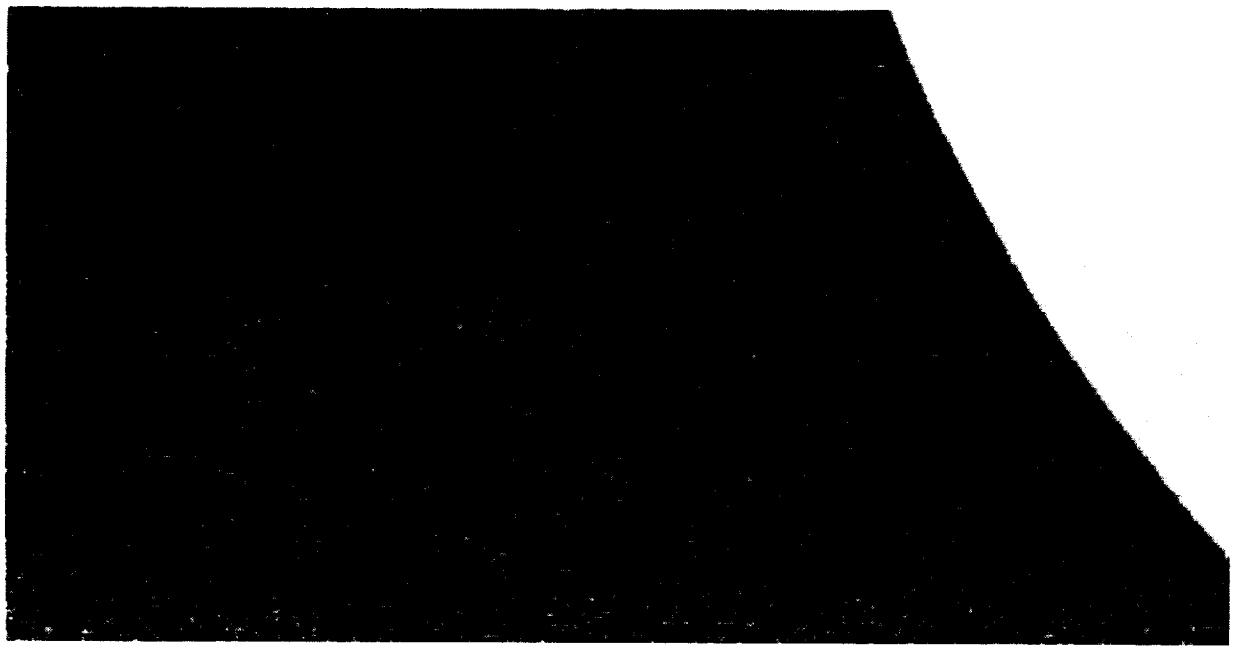

Figure 3. Illustration of JPL type B noise.

Figure 4. Illustration of JPL type C noise.

Two of the same type images were always presented side by side using the psychological method of "pair comparisons" (ref. 7). The images varied only in terms of their quantization level and position (left or right side). The evaluator did not know what quantization levels were applied to the images. The test images were approximately 7 in. (width) × 9 in. (height).

Software development: The number of images displayed was on the order of hundreds because of the need to present four q tables and numerous quantization steps. A software script was written to automate the experiment and help avoid human error. It also ensured uniformity across the three test stations, facilitated a smooth and seamless data collection session, provided more flexibility (with respect to making last minute changes to the testing schedule), and allowed for automatic recording of trial data. The software controlled: (1) image retrieval, (2) image cropping and enlarging, (3) image q table and

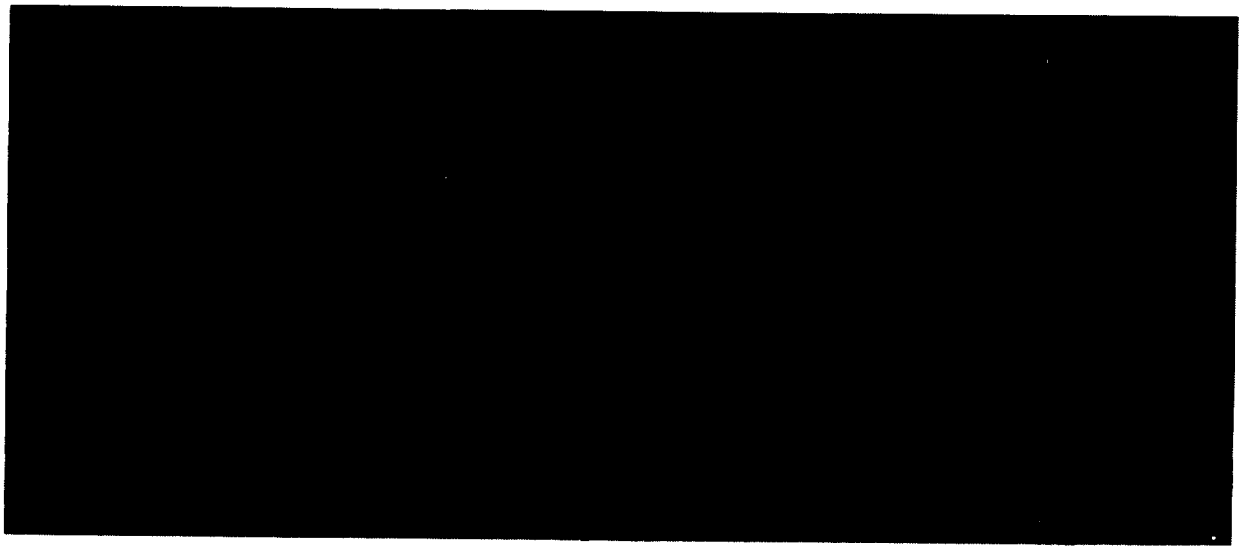

Figure 5. Illustration of JPL type D noise.

compression level application, and (4) evaluator keyboard responses.

The software script used the evaluator identification (ID) as a parameter and executed the file using data from two easily editable data files. The first file contained all image files assigned to the evaluator. The second file contained the information needed for image display (cropping and magnification and q table data to be applied). The software script selected the appropriate image, cropped it, compressed and reconstructed the cropped area using the appropriate q table, and displayed it on the screen. The script prompted the experimenter to enter the q-factor range (step sizes) for each set of images. The range was determined on an a priori basis for the first evaluator's trials (typically 2 to 36) within a common image type group and subsequently by the visual judgments of previously tested evaluators using progressive division.

Following each test session, the software script prepared and displayed all combinations of compressed images assigned to an evaluator ID and printed the evaluator's recorded responses. The printout was used to decide which q levels to use with the next evaluator within the same image type group and to make possible a rapid preliminary data analysis.

Evaluators and their institutions– Fifteen people took part in the experiment. Six of them were SSI team members (representing six different institutions) and the remaining nine were workshop attendees from nine other institutions. Thirteen pretest survey respondents participated in the image evaluations (representing six different institutions). Last minute schedule changes during the workshop required that the new group of volunteers agree to evaluate image classes that they may or may not be particularly qualified to judge. In addition, they were not given an opportunity to preselect the type of images they would be shown.

Table 4 lists the evaluators' institutions, SSI team status, vision correction, and information about the image classes presented to them.

Results

Acceptability results by image type and q table– Only four of the fourteen image types studied are presented in this section to illustrate the findings and the presentation format used. The remaining images are in appendix H.

Data for each of the four image types are presented with corresponding test results for each q table and evaluator. In addition, observations are presented within each section dealing with that image type. The levels tested are displayed at the top of each figure. The score, at the bottom of the figure, represents the total number of acceptable ratings (A) minus the total number of unacceptable ratings (N) for each quantization level. Since each evaluator was presented three pairs of images (at three q levels in different left–right orders) for each image type, there were six opportunities to rate each image. There are a total of six As and/or Ns shown above and/or immediately below each evaluator's dashed line. A pair of As or Ns above and below the line is expected and indicates a constant rating of the same level. An A–N pair side by side indicates that the evaluator's rating was not based upon a well-defined criterion so that he or she split

Table 4. Test subject testing details.

Institution	SSI team	Vision	Image 1	Image 2	Image 3	Image 4
Ames Research Center	2	c	Solid + limb r.6.r	Noise rq538.g.r	Solid + no limb r.4.r	Noise r6.noise.r
RAND Corporation	3		Solid + limb r.6.r	Noise r.6noise.r	Solid + term. r.1.r	
Geological Survey	1		Solid + limb r.6.r	Noise r.6noise.r	Solid + term r.1.r	
Lunar Planetary Laboratory (University of Arizona)		c	Solid + limb r.9.r		Solid + term r.1.r	--
University of Hawaii	2		Solid + limb r.9.r	Solid + no limb sr7.raw.r	Solid + limb r.6.r	Noise r6.noise.r
Jet Propulsion Laboratory	4		Solid + limb r.9.r	Solid + term. r.1.r	Small bodies rq538.gas.r	--
U.S. Geological Service	1	c	Solid + no limb r.4.r	Noise rq538.g.r	Solid + no limb sr.7raw.r	Noise sr7.noise.r
Ames Research Center	3	c	Gas + no limb	-- r.14.r	Gas + no limb r.15.r	Gas + no limb rq538.j4o.r
York University	3	c	Solid + no limb	Noise sr7.raw.r	Small bodies sr7.noise.r	-- rq538.gas.r
Jet Propulsion Laboratory (Multimission Image Processing Laboratory)	--		Solid + no limb r.4.r	Noise rq538.g.r	Solid+term. r.1.r	--
ITRES Research Ltd.	1	c	Gas + no limb	Noise r.15.r	Dark side rq538.j4o.r	-- rq538.litn.r
Institute for Space and Terrestrial Science (York University)	1		Gas + no limb r.15.r	Noise rq538.j4o.r	Dark side rq538.litn.r	Gas + no limb r.14.r
National Optical Astronomy Observatory	1	c	Dark side	-- rq538.litn.r	Rings r.11.r	Small bodies rq538.gas.r
California Institute of Technology	2	c	Rings r.11.r	--	Gas + no limb r.15.r	Gas + no limb rq538.j4o.r
Cornell University	2		Gas + no limb	-- r.14.r	Gas + no limb r.15.r	Rings r.11.r

1 = SSI team member; 2 = interdisciplinary scientist; 3 = site manager; 4 = exp. representative;
c = vision corrected with glasses.

their acceptance rating each time. Each A rating was arbitrarily located just to the left and each N score just to the right of a vertical line through that q level. All scores given here represent an integration of all evaluators' selections of an acceptable image usefulness (a score of 3 or greater). To help smooth out the data and take away the biasing influence of (possibly) large individual differences among the evaluators the scores shown were interpolated in the following way.

If an evaluator consistently rated the image as acceptable (e.g., app. H, fig. H-2(b), subject 3 on page 49), scores of A were assumed for all lower and intermediate levels tested (to reduce visual clutter not all q levels are shown). Likewise, if an evaluator consistently rated that image to be unacceptable, as subject 2 did in the same figure, scores of N were assumed for all higher and intermediate levels tested. In order to combine these evaluations an A is valued 1 and an N as –1. Thus, at q = 2 there were 3 As and 3 Ns for a final score of 0. This testing procedure was based on the assumption that if each evaluator had been presented with the other quantizations their ratings would have been consistent.

In order to support further hypothesis testing by the reader figure 6(a) shows the surface of Europa (uncompressed) along with the raw data obtained for this image (cf. fig. 6(b)–(d)). The safe and (most) likely range of levels (and corresponding compression levels) were determined by noting where the acceptable rating scores crossed from positive to negative. When the score changes from positive to negative over two or three levels the safe and likely range values given are the same. When scores exhibit a less clearly defined or more variable positive to negative crossing, the safe q range cited represents the more conservative of the two q levels (e.g., fig. H-2(b)). In figure 6(b), for instance, the safe and likely q range of appeared to be in the 18–23 region, dropping through zero at q = 19. Perhaps a clearer example is shown in appendix H, figure H-4(b), where the number of acceptable ratings varied from 4 at q = 10 to 0 at q = 14 to – 4 at q = 18. A safe and likely q range of 10–18 is indicated here (corresponding to a compression ratio of 4:1 to 8:1, respectively).

Providing a range of values was preferable to citing a single value since the evaluators' ratings were spread over a range of levels. Each evaluator looks for different image features and applies slightly different evaluation criteria. Nevertheless, relatively consistent rating scores were obtained for the majority of cases.

Shown on the right side of each raw data figure are two columns labeled A and B. In column A, an "N" means the evaluator was not preselected to be a test participant on the basis of the pretest survey. A "Y" means the evaluator was preselected. The possible significance of this is that the N evaluators volunteered to be tested at the time of the workshop and may or may not have been particularly qualified to examine and rate the images presented. The practical impact of this selection factor remains to be seen. In column B the number represents the rating (from 1 to 5) the evaluator gave to the uncompressed image displayed before testing began. Recall that, to help the evaluators establish a relatively stable evaluation rating criterion, they were shown an uncompressed example of the image. Thus, they knew that the initial image was as good as the set of images to follow was going to be. Therefore, they were able to give the uncompressed image a numeric score from 1 to 5. The great majority of these scores are fours and fives, as expected. Now we will turn to the data.

Solid surface with limb: Two images without noise (r.6.r, Europa; r.9.r, Io) were presented to test this image class. In addition, file r6.noise.r was presented. It consisted of file r.6.r with superimposed type B noise. Following are the results for file r.6.r. to illustrate how these data are presented. The last two files are presented in appendix H.

The acceptable compression range was moderately high (typically ranging from 4:1 to 20:1) for this image across these q tables. The values are most likely the result of the ICT algorithm's processing of moderately fine spatial detail network present on this surface. Use of q table 0 produced the highest acceptable ICT compression (12:1–20:1). Interestingly, all three q tables produced approximately the same range of safe and likely compressions.

Figure 6. (a) Image file r.6.r (Europa).

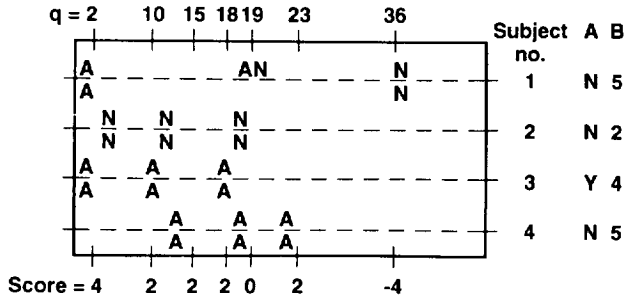

Safe range 18 - 23 **Compression ratios 8 - 12**
Likely range 18 - 23 **Compression ratios 8 - 12**

Figure 6. (b) File r.6.r (Europa) using q table 0.

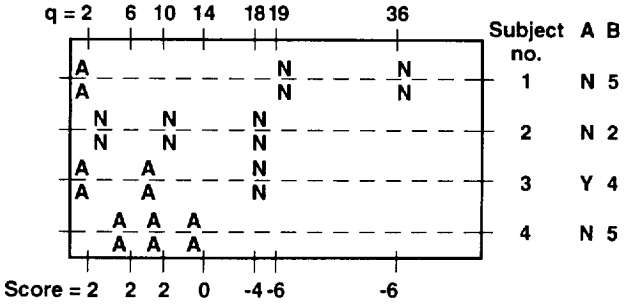

Safe range 10 - 18 **Compression ratios 9 - 15**
Likely range 10 - 18 **Compression ratios 9 - 15**

Figure 6. (c) File r.6.r (Europa) using q table 1.

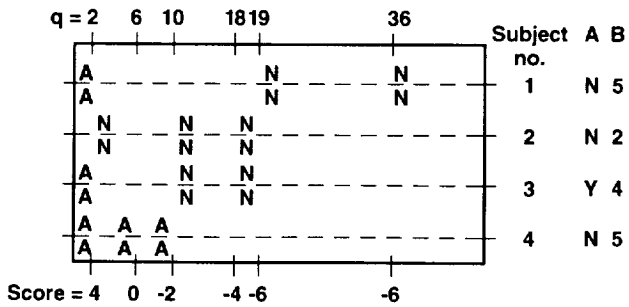

Safe range 2 - 10 **Compression ratios 4 - 12**
Likely range 6 - 10 **Compression ratios 8 - 12**

Figure 6. (d) File r.6.r (Europa) using q table 2.

Solid surface without limb: Two images without noise (r.4.r; sr7.raw.r) and two with noise (rq538.g.r; sr7.noise.r) were studied in this image class. The first of these four images is presented here with the other three presented in appendix H. Three evaluators rated them with the following results.

As figure 7(a) shows, this no noise, solid surface without limb image is characterized by linear and curvilinear surface details varying in both size and contrast. The largest acceptable compression range from (8:1 to 12:1) q table 2; q table 0 yielded the next largest values from (9:1–10:1). These relatively small ranges of acceptable compressions indicate that the evaluators employed a fairly precise and stable criteria for judging the imagery, as would be expected if they were looking for high spatial frequency image detail.

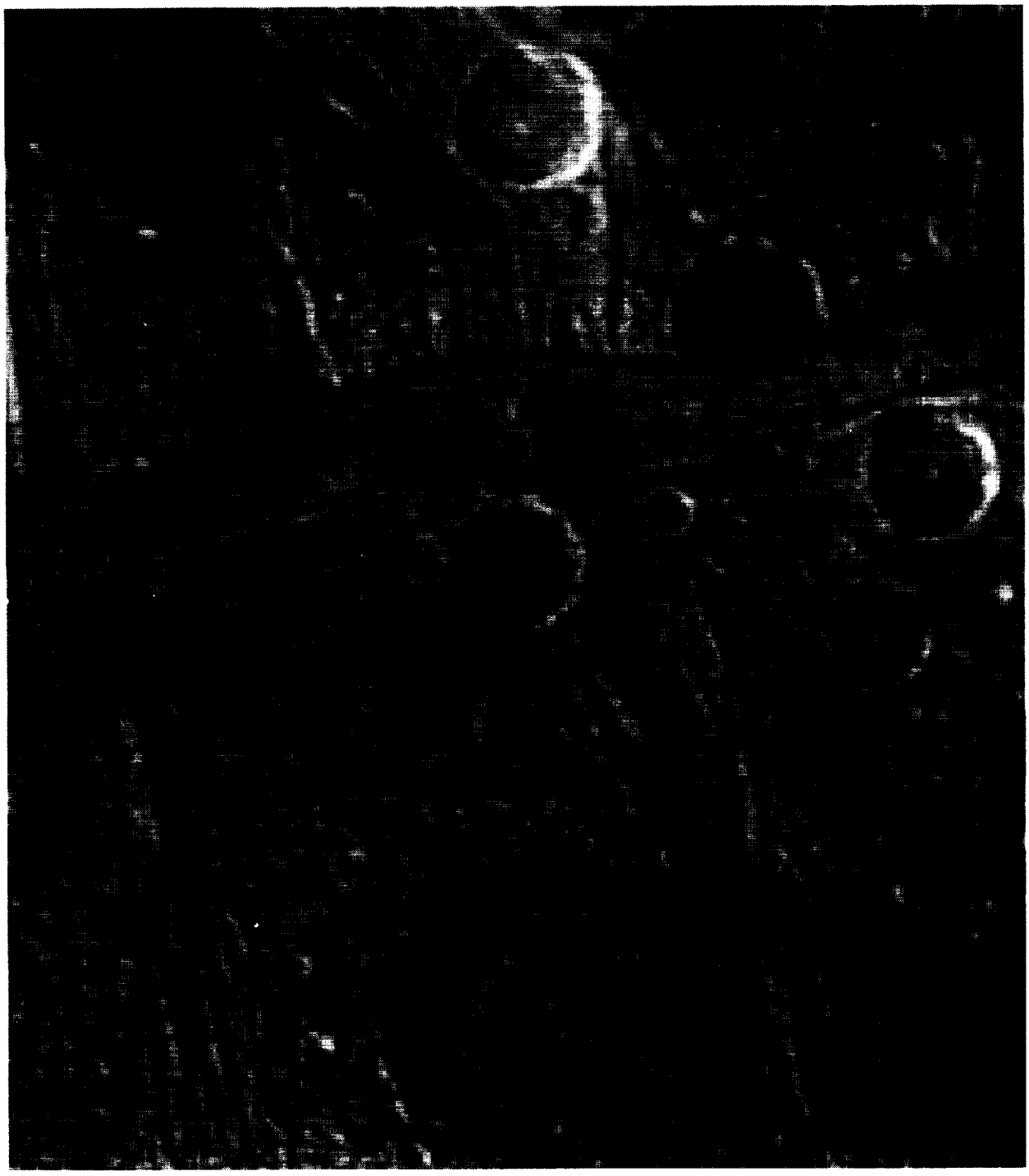

Figure 7. (a) Image file r.4.r (Ganymede).

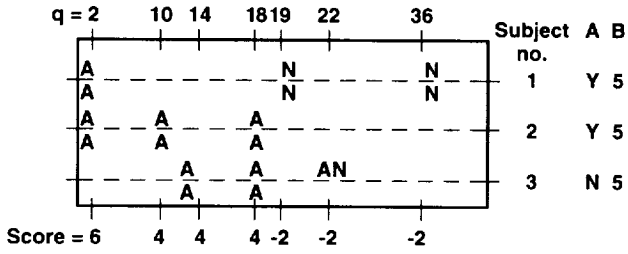

Safe range 18 - 19 Compression ratios 9 - 10
Likely range 18 - 19 Compression ratios 9 - 10

Figure 7. (b) File r.4.r (Ganymede) using q table 0.

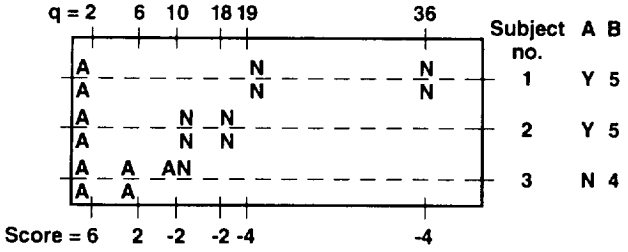

Safe range 6 - 10 Compression ratios 6 - 9
Likely range 6 - 10 Compression ratios 6 - 9

Figure 7. (c) File r.4.r (Ganymede) using q table 1.

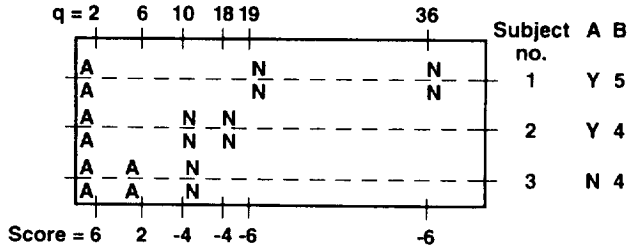

Safe range 6 - 10 Compression ratios 8 - 12
Likely range 6 - 10 Compression ratios 8 - 12

Figure 7. (d) File r.4.r (Ganymede) using q table 2.

Gaseous surface without limb: Three images of Jupiter were studied in this category (r.14.r; r.15.r; and rq538.j4o.r). Three observers rated the first image, five the second image, and two the third image. File r.14.r is found in appendix H. Files r.15.r (without noise) and rq538.j4o.r (with noise) are presented here.

Figure 8(a) is composed of medium to low contrast amorphous gaseous regions with "soft boundaries" that can be compressed with relatively great efficiency. Acceptable compression ratios as great as 57:1 were found for q table 2.

Figure 8. (a) Image file r.15.r (Jupiter) without noise.

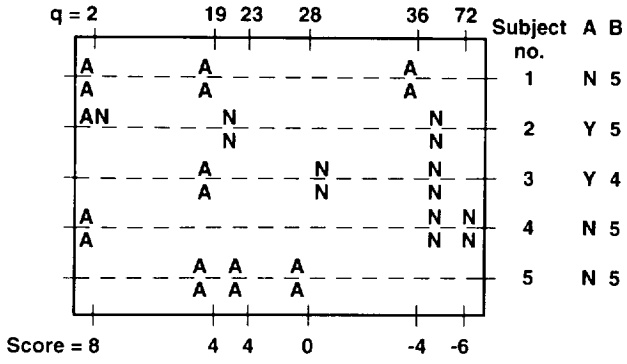

Safe range 23 - 36 Compression ratios 36 - 53
Likely range 23 - 36 Compression ratios 36 - 53

Figure 8. (b) File r.15.r (Jupiter) using q table 0.

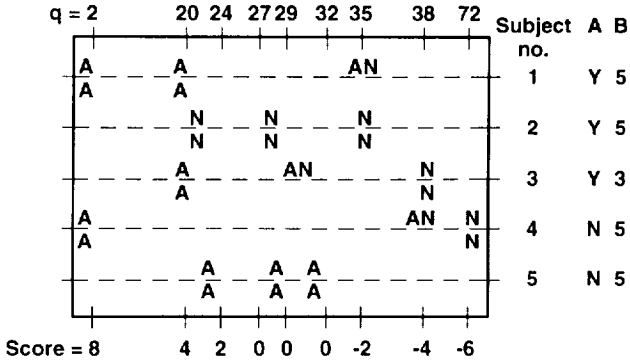

Safe range 24 - 35 Compression ratios 42 - 57
Likely range 24 - 35 Compression ratios 42 - 57

Figure 8. (c) File r.15.r (Jupiter) using q table 2.

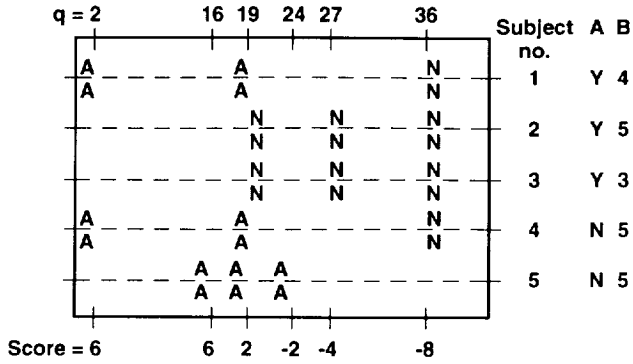

Safe range 19 - 24 Compression ratios 48 - 53
Likely range 19 - 24 Compression ratios 48 - 53

Figure 8. (d) File r.15.r (Jupiter) using q table 3.

Results for figure 9(a) may be compared with the results for the identical image without noise (fig. 8(a)). For q table 0 the presence of noise reduces the safe and likely ranges of acceptable ICT compression from 36:1 to 53:1 down to only 1:1. For q tables 2 and 3 a correspondingly large negative noise effect is found on acceptable compression ratios. The greatest acceptable compression (6:1) is provided by q table 3 and is approximately a factor of only 8 times worse than the corresponding q table 3 for the same image without noise (fig. 8(d)). Using q table 0 with this noisy image yields as much as 53 times worse compression compared to its no noise counterpart (fig. 8(b)). Likewise, using q table 2 with this noisy image yields as much as 19 times worse compression compared to its no noise counterpart image (fig. 8(c)).

Table 5 summarizes the results by image type, file designation, and q table.

Figure 9. (a) Image file rq538.j4o.r (Jupiter) with noise.

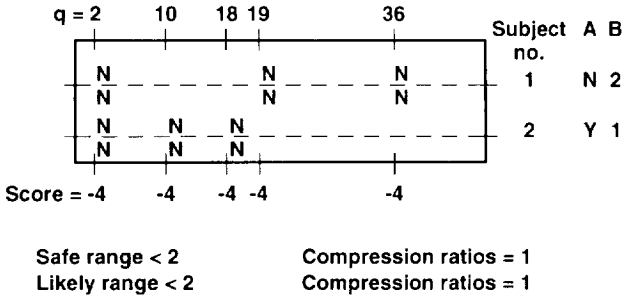

Figure 9. (b) File rq538.j4o.r (Jupiter) using q table 0.

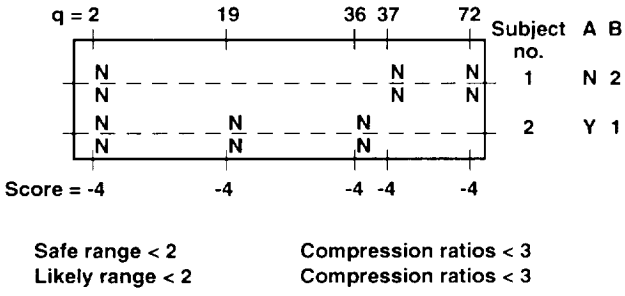

Figure 9. (c) File rq538.j4o.r (Jupiter) using q table 2.

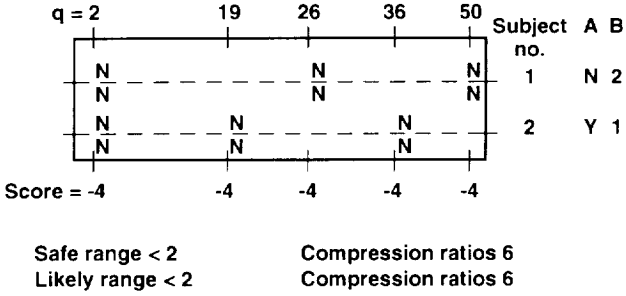

Figure 9. (d) File rq538.j4o.r (Jupiter) using q table 3.

Selected comments made by evaluators–Some evaluators made comments during and after the data collection period that shed light on some of the cognitive processes they used to evaluate these images. Some participants were not particularly interested in helping to generate these data because they rarely do visually based examinations or quantification of such images in their laboratories. One evaluator remarked several times during data collection, "I would have stretched this image," and "I am only interested in dark-side phenomena."

The percentage value given below was his estimate of the degree of correspondence between the "morphological shapes/structures" application listed with image class (e.g., gaseous with limb (95%); gaseous without limb (95%); dark-side phenomena (lightning, meteors) (90%). It was suggested that we present two images exactly superimposed and present them alternately to better (visually) demonstrate their differences due to compression.

One evaluator remarked, "I'm not interested in the appearance of images but in the preservation of the luminance array . . . its statistical characteristics. If we have a limited downlook and are interested in the surface's radiometric characteristics, what is the trade-off between spatial resolution and luminance? I am interested in finding out what effect the ICT compression will have on my ability to measure true edges, edge distortion."

Another evaluator who normally analyzes images only photometrically said, "My rating depends on what I am doing. I can't judge the photometric quality (of these images). All (of these) images are very bland. We never look at images this way. My judgments go to hell with all images that I detect as being compressed."

Table 5. Summary of acceptable image quality compression results by type of image

Image type	File		q = 0	q = 1	q = 2	q = 3	Figure
Solid surface with limb	r.6.r	Safe	8–12	9–15	4–12		6(a)
		Likely	8–12	9–15	8–12		
	r.9.r	Safe	37–42	35–46	44–46	--	H-1(a)
		Likely	37–42	41–46	44–46	--	
	r6.noise.r	Safe	1–5	<2	<3	--	H-2(a)
		Likely	4–5	<2	<3	--	
Solid surface without limb	r.4.r	Safe	9–10	6–9	8–12		7(a)
		Likely	9–10	6–9	8–12	--	
	sr7.raw.r	Safe	>38	23–41	23–36	--	H-3(a)
		Likely	>38	29–41	32–36	--	
	rq538.g.r	Safe	4–8	<3	<4	--	H-4(a)
		Likely	4–8	<3	<4	--	
	sr7.noise.r	Safe	1	<2	<2	--	H-5(a)
		Likely	1	<2	<2	--	
Solid surface with terminator	r.1.r	Safe	11–17	12–15	11–18	--	H-6(a)
		Likely	11–17	12–15	11–18	--	
Gaseous surface without limb	r.14.r	Safe	55–67	51–71	54–72	--	H-7(a)
		Likely	55–67	51–62	54–72	--	
	r.15.r	Safe	36–53	--	42–57	48–53	8(a)
		Likely	36–53	--	42–57	48–53	
	rq538.j4o.r	Safe	1	--	<3	6	9(a)
		Likely	1	--	<3	6	
Small bodies	rq538.gas.r	Safe	35–61	37–50	36–54	--	H-8(a)
		Likely	35–61	37–50	36–54	--	
	rq538.litn.r	Safe	71–75	80–86	83–88	--	H-9(a)
		Likely	71–75	80–86	83–88	--	
Rings	r.11.r	Safe	>36	>45	>48	--	H-10(a)
		Likely	>36	>45	>48	--	

DISCUSSION

SSI team members preprocess the imagery they study in various ways before they study it visually. This is done, among other reasons, to enhance certain features (e.g., through contrast enhancement or luminance stretching). For purely practical reasons each evaluator was not able to do preprocessing before viewing and judging the images during this study. This may limit the applicability of the data. Nevertheless, the data provides some useful insights into the relative magnitude of acceptable compression ratios for different classes of images, noise types, quantization matrices, and levels presented.

The data were placed into low, medium, and high acceptable image ICT compression ratio groups. The low acceptable compression ratio group was arbitrarily defined as ranging from no compression (1:1) to between 4:1 to 8:1. The four images with superimposed noise (the solid with limb, solid with no limb, and gaseous with no limb classes; table 2) fell into this group regardless of which q table was used. As expected, the presence of radiation noise played an important role in reducing the effectiveness of the ICT algorithm in yielding an acceptable image. Noise type C (fig. 4) yielded the greatest acceptable compression (from 4:1 to 8:1). Noise types B and D yielded data that could not be compressed

without making the image unacceptable. Because not all types of images were cross-compared with all noise types it is not possible to say whether the noise alone or its interaction with certain kinds of image detail produced the unacceptable results. A systematic parametric study should be reserved for future study to relate different image features and superimposed noise to maximum acceptable image compression.

There were three images in the medium acceptable compression ratio group from 8:1 to 17:1; r.6.r (fig. 6(a)), r.4.r (fig. 7(a)), and r.1.r (fig. H-6(a)). All images are solid surface and are characterized by the presence of high spatial frequency detail such as craters, linear structures, and other varied shapes of medium to high contrast.

The greatest acceptable ICT compression ratio group was, on the basis of the present results, arbitrarily defined as greater than 35:1. Six images fell into this group. They are relatively diverse in image detail and deserve separate discussion. Image r.11.r (fig. H-10(a)) was the dark side of Saturn with a bright terminator/limb and a portion of rings visible on the lower right side. A small plume and several small bright points of light are also visible. The q tables 0, 1, and 2 yielded acceptable compressions of >36:1, >45:1, and >48:1, respectively.

Image r.9.r (fig. H-1(a)) was the clear surface of Io with limb, at least one large plume, active volcanoes, lava flows, collapsed caldera, and craters. Acceptable ICT compression ratios were as high as 46:1 using q table 2. The q table 0 and 1 also elicited relatively high compression ratios. The dark sky background was cropped significantly to permit visual inspection both of the sky around the plume and part of Io's surface while reducing the amount of dark sky present.

Images sr7.raw.r (fig. H-3(a)) and r.15.r (fig. 8(a)) were both no-limb/no-noise images and yielded relatively high acceptable compression ratios (from 36:1 to 53:1) using q table 0. However, sr7.raw.r was a solid surface image of Io with broad plains, hills and mountains, and other large scale features, while r.15.r was an image of the gaseous surface of Jupiter with low- to medium-contrast amorphous cloud patterns.

Image r.14.r (fig. H-7(a)), the gaseous surface of Jupiter without limb, showed the (dark) red spot with bands of swirling lighter clouds around it. The range of acceptable compression ratios ranged from 51:1 to 72:1. The highest acceptable compression was associated with q table 3.

Image rq538.gas.r (fig. H-8(a)) was cropped closely around the boundary of the asteroid's top, right, and bottom sides. Its high-contrast irregular surface detail and terminator yielded acceptable ICT compression ratios (from 35:1 to 61:1).

As anticipated, the highest acceptable ICT compression ratios were associated with image rq538.litn.r (fig. H-9(a)). This image has an almost homogeneously dark surface with multiple small bright spots (lightning phenomena). The three evaluators who rated the image said it was acceptable as long as they could see and count a certain number of these multi-pixel (lightning) spots. The ICT algorithm and/or the q tables may have altered the visual detectability of some of the lower-contrast spots. This type of limited judging criteria results in a less than acceptable basis to actually apply the results.

Many of the SSI team members reported their evaluations of compressed versions of the sample images at the workshop. However, most did not identify an acceptable level in a manner suitable for comparison to our methodology. A limited comparison can made with only two reports.

First, researchers at the Planetary Science Institute (ref. 8) evaluated compressed images of Gaspra (rq528.gas.r, fig. H-2(a)). They concluded that significant scientific information was lost for ICT compression with linear levels of 8 or more and recommended no compression for their observation interests. However, in our experiment three subjects viewed the compressed Gaspra image and the results are presented in figure H-8(b)–(d). These subjective evaluations indicate linear quantization (q table 0) of 28 to 45 and yield acceptable compression ratios from 35:1 to 61:1.

Second, researchers at the Department of Geology, Arizona State University (ref. 9), assessed the discernability of geologic features as a function of ICT level for several satellite images. Four of the images (R1, R4, R6, and R9) were the same as the sample images used in our experiment, thus a direct comparison can be made. Only the linear table was used corresponding to q table 0 in our experiment. The correlation of results is mixed. For Callisto (R1; fig. H-6(a)–(d)), researchers' limiting quantization is about twice as high as the safe range in our study (11 to 16 versus our 5 to 7). For Ganymede and Europa (R4 and R6; figs. 6(a)–(d) and 7(a)–(d)), the researchers' limiting quantization is similar, but slightly more restrictive than our safe range (11 to 16 versus our 18 to 23). For Io (R9, fig. H-1(a)–(d)) the researchers' limiting quantization is less than half our safe range (16 versus our 36 to 45).

These comparisons suggest that there is considerable variance in what is considered acceptable quantization to a researcher. Subjective visual acceptability should not be used alone to set the ICT level for any given image.

It is not possible to estimate with any accuracy beforehand the degree to which a given no-noise image can be compressed and still yield a useful image using the ICT algorithm and q tables. Individual differences in scientific background, discipline, and practical experience

of the evaluators probably account for most of the response variance. Unfortunately, there was not enough data collected to permit an analysis of variance to be performed to determine the influence of such factors.

Considering the influence of the four q tables studied (table 5), q table 0 yielded the greatest acceptable ICT compression in 4 (28%) of the 14 images studied (r6.noise.r, fig. H-2(a)); sr7.raw.r (fig. H-3(a)); rq538.g.r (fig. H-4(a)); rq538.gas.r (fig. H-8(a)). Image sr7.raw.r could be compressed to a relatively high degree (>38:1), but the other image rq538.g.r (fig. H-4(a), most likely because of the presence of noise, only to a relatively low degree (8:1). The q table 1 yielded the greatest acceptable compression ratio (from 9:1 to 15:1) in only 1 (7%) of the 14 images (r.6.r, fig. 6(a)). The q table 2 yielded the greatest acceptable ICT compression in the remaining 8 (57%) of the 14 images studied.

GENERAL CONCLUSIONS

Radiation noise significantly reduces acceptable ICT compression rating scores particularly when high spatial frequency information is present. Radiation noise also degrades low spatial frequency information if the ICT compression used also eliminates high-frequency information. These results also show that it is not possible to predict on an a priori basis whether a given type of image will be rated as acceptably useful when compressed to some prespecified level using the ICT algorithm and q table. Indeed, while there may appear to be a some amount of redundant information within a given image (which might be considered as candidate for elimination by the compression algorithm) such information may still be important from a visual evaluation standpoint to some investigators. Until much more knowledge and insight is available about how the human visual system processes and interprets different kinds of image characteristics and how different cognitive processing factors within different investigators interact with the image compression parameters used, we will need to continue to perform psychophysically based image evaluation rating studies using highly experienced evaluators following clearly defined and consistently applied testing instructions.

Ames Research Center
National Aeronautics and Space Administration
Moffett Field, California
March 23, 1994

REFERENCES

1. Belton, M. J. S., et al: The Galileo Solid-State Imaging Experiment. Space Sci. R., vol. 60, no. 1–4, May 1992.
2. Cham, W.: Development of Integer Cosine Transforms by the Principle of Dyadic Symmetry. IEEE Proc., vol. 136, pt. 1, no. 4, Aug. 1989.
3. Cheung, K-M.; and Tong, K.: Proposed Data Compression Schemes for the Galileo S-band Contingency Mission. 1993 Space and Earth Science Data Compression Workshop, Snowbird, Utah, April 2, 1993, NASA CP-3191, pp. 99–109.
4. Ekroot, L.: Preliminary ICT Compression Performance on Galileo Images. Jet Propulsion Laboratory, Interoffice Memorandum 331-93.2-042, June 4, 1993.
5. Rabbani, M.; and Jones, P. W.: Digital Image Compression Techniques. SPIE Optical Engineering Press, vol. TT7, 1991, pp. 108–111.
6. Haskell, B. G.; and Steele, R.: Audio and Video Bit-rate Reduction. IEEE Proc., vol. 69, no. 2, Feb. 1981, pp. 252–262.
7. Guilford, J. P.: The Method of Pair Comparisons. Psychometric Methods, McGraw-Hill, 1954, pp. 154–177.
8. Chapman, C. R.; Ryan, E. V.; Merline, W. J.; and Howell, S. B.: Craters and Geological Features as Affected by Noise and Image Compression: Studies using Galileo SSI Images of Gaspra. Presented at Galileo SSI Workshop on Image Compression, Ames Research Center, Moffett Field, Calif., July 22, 1993.
9. Sullivan, R.; Bender, K.; Pappalardo, R.; and Greeley, R.: Effects of ICT Compression on Geological Analysis. Presented at Galileo SSI Workshop on Image Compression, Ames Research Center, Moffett Field, Calif., July 22, 1993.

APPENDICES

A. Integer Cosine Transform

Cham (ref. 2) proposed the integer cosine transform (ICT). The ICT requires only integer multiplication and additions. All elements in the ICT matrix are integers with sign and magnitude patterns that resemble those of the discrete cosine transform (DCT) matrix. Relatively fast ICT computations (and their inverse processes) are supported because of two factors: (1) the orthogonality property of the ICT ($CC^t = \delta$, where C is an ICT matrix and δ is a diagonal matrix, and (2) ICT's similarity to the DCT matrix.

Later, Cheung and Tong (ref. 3) proposed a modification to Cham's ICT that permitted generalization to any N-point ICT. It is this modification that was employed here. According to Cheung and Tong:

Let C and A be the respective ICT and DCT $N \times N$ matrices. $A = (a\ kn)$ is an orthonormal matrix ($AA^t = I$) defined as:

$$a\ kn = 1/\sqrt{N} \qquad k = 0, \qquad 0 < n < N-1$$

$$= \sqrt{2/N}\cos\frac{\pi(2n+1)k}{2N}$$

$$1 < k < N-1, 0 < n < N-1 \qquad \text{(A-1)}$$

Using A as a template, the ICT matrix $C = (c\ kn)$ is an orthogonal matrix ($CC^t = \delta$, where δ is a diagonal matrix) with the following properties:

1. Integer property: c kn are integers for $0 < k, n < N-1$
2. Orthogonality property: rows (or columns) of C are orthogonal.
3. Relationship with DCT:
   (a) sgn (c kn) = sgn (a kn) for $0 < k, n < N-1$
   (b) If a kn = A st, then c kn = Cst for $0 < k, n, s, t < N-1$.

B. Quantization Table Values

These values were provided by A. B. Watson of Ames Research Center.

q0	8	25	18	25	8	25	18	25
	25	78	56	78	25	78	56	78
	18	56	40	56	18	56	40	56
	25	78	56	78	25	78	56	78
	8	25	18	25	8	25	18	25
	25	78	56	78	25	78	56	78
	18	56	40	56	18	56	40	56
	25	78	56	78	25	78	56	78
q1	8	25	18	25	16	75	89	200
	25	78	56	156	50	234	279	702
	18	56	40	112	36	223	240	559
	25	156	112	156	75	312	391	936
	16	50	36	75	32	150	179	425
	75	234	223	312	150	702	782	1950
	89	279	240	391	179	782	920	2234
	200	702	559	936	425	1950	2234	5460
q2	8	25	18	50	24	175	286	1099
	25	78	56	156	100	546	950	3666
	18	56	80	168	89	503	880	3296
	50	156	168	312	175	1092	1787	6786
	24	100	89	175	96	600	984	3722
	175	546	503	1092	600	3666	6144	19890
	286	950	880	1787	984	6144	10200	14244
	1099	3666	3296	6786	3722	19890	14244	19890
q3	8	25	36	125	128	1898	4562	6370
	25	78	112	468	475	7098	14244	19890
	36	112	160	559	572	8490	10200	14244
	125	468	559	1794	1898	19890	14244	19890
	128	475	572	1898	2040	6370	4562	6370
	1898	7098	8490	19890	6370	19890	14244	19890
	4562	14244	10200	14244	4562	14244	10200	14244
	6370	19890	14244	19890	6370	19890	14244	19890

C. Pretest SSI Member Survey Instructions and Forms.

Information Sciences Division
Spacecraft Data Systems
Research Branch

To: SSI Team Members

From: Sherry Chuang
Ames Research Center
Spacecraft Data Systems Branch (Code FIS)
Remote Payload Systems Research Group Leader

Date: June 23, 1993

Re: Questionnaire on Galileo S-Band Mission Image Requirements

Ames Research Center is supporting JPL in assessing the quality of images based on the planned ICT image compression algorithm for the Galileo S-band mission. Our role is to survey the SSI team members to understand the scientific features of interest in the images that are expected back from the SSI camera sensors, and then conduct an empirical, subjective quality assessment of a variety of compressed images. The information collected in the survey of the SSI team will be incorporated into an unbiased controlled experiment that will be conducted at the July 22 Workshop at Ames.

As a member of the SSI team, your input is very important to us regarding your imaging requirements. We need to understand what images you are planning to use, how you plan to use your images, and what pre-processing requirements you have in order for us to help JPL derive optimal compression algorithm parameters. We recognize that algorithm design and associated quantization tables may impact how effectively you will be able to process certain image features later. Please fill out the attached questionnaire to help us plan a productive image evaluation session at the Workshop.

We have sent a set of questionnaires to all SSI PIs, site managers and associate scientists. If you have any questions about the directions or appropriate responses, please call or send e-mail to :

Dick Haines, 415-604-3376, dick_haines@styx.arc.nasa.gov
Yaron Gold, 415-604-3512, yaron@ptolemy.arc.nasa.gov

Fax the questionnaire to Dick Haines/Yaron Gold at fax # 415-604-3594 by July 1.
Thank you for your cooperation.

Galileo SSI Team Survey Instructions

1. Introduction

Based upon a pilot phone survey we have identified a set of image analysis applications (or operations) for which the SSI Team members intend to use the Galileo images. This is probably not an exhaustive list, nor is any one team member likely to use all applications. From this survey we hope to find out how individual team members view the relationship between these applications to (A) various types of images, and to (B) certain image properties which will be affected by compression. We expect these relationships to vary between team members.

2. Form Layout

The list of image analysis applications is in the middle column, under the label "APPLICATIONS". The two other columns (labeled **A. Image Classes** on the left, and **B. Spatial- vs. Gray-Scale Resolution** on the right) are used to describe the two kinds of relationships. For the purpose of this survey we divided the applications into three groups. Two of the groups, **I. Visual information extraction** (looking at the image), and **II. Photometric Operations** (manipulating actual data numbers), have corresponding matrices both on the left (**A1, A2**) and on the right (**B1, B2**). The third group, **III. Image Pre-processing** (software operations employed before the applications in groups I and II) only has a corresponding matrix on the left (**A3**). Each application group has room (labeled "Other:...") for adding an application we have not included.

3. Instructions

- Fill out the requested information in the lower right corner of this form .

- In the column labelled **Applications** circle the letter of each application that is relevant to your work List others if necessary.

A. Image Class

Use Matrices **A1, A2,** and **A3.** Each column of these matrices corresponds to one of seven basic classes of ***Galileo Images*** (e.g., small bodies, solid [surface] with limb, gaseous [Jupiter] without limb, etc.). Representative examples of all seven image classes are enclosed (**Figure 1**) to help illustrate what we mean. If you feel that you require an additional category add it in the column labelled "Other..." and breifly describe it on the back of the survey form.

Specific Directions for Image Classes:

- (A) For each **Application** you circled in group **I. Visual Information Extraction** go across to the left and determine which image class (or classes) is (are) relevant to this application. Make a circle around the appropriate box of matrix **A1** (leave room inside the box - later you will enter a number there).

- (A') For each column (image class) in matrix **A1**, rank the boxes you circled in step (A) with respect to the significance of the application to the image class. Do this by inserting a percentage score in the circled box. The higher the score, the more significant the application to this type of image. The scores in any given column must add up to 100 percent.

- (A") Repeat steps (A) and (A') for Application Groups **II** and **III**. Use Matrices **A2** and **A3**, respectively.

A. Image Classes

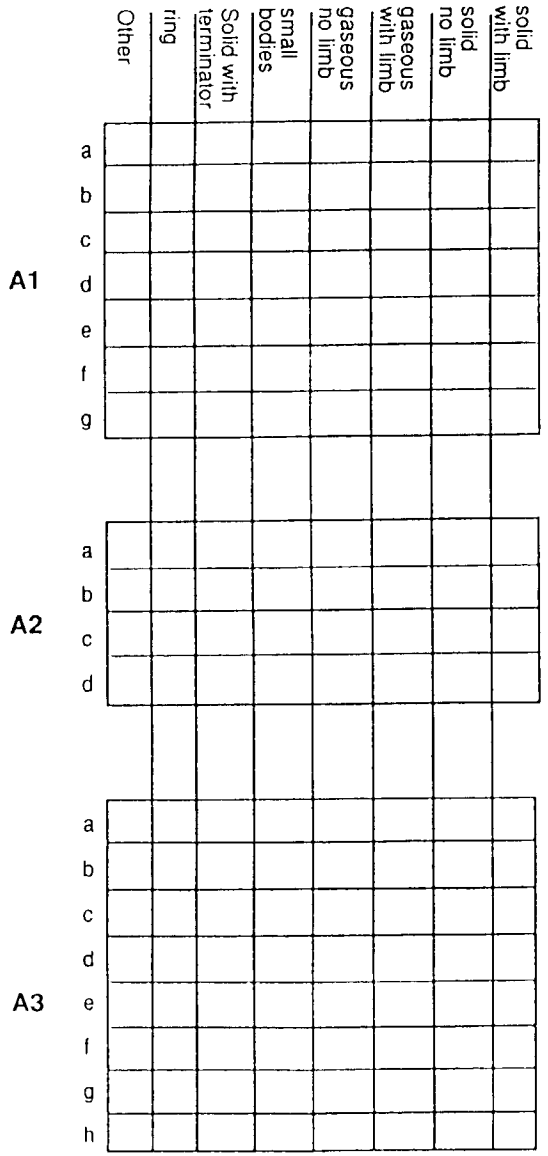

APPLICATIONS

I Visual Information Extraction

a. Morphological Shapes/Structures

b. Horizontal Distance Measurement

c. Textures and Patterns

d. Region Boundaries

e. Topography (Relief) from shadows

f. Depth from Stereopsis

g. Other: _____

II Photometric Operations

a. Reflectance Measurements

b. Shape-From-Shading

c. Multi-Spectral Ratios

d. Other: _____

III Image Pre-processing

a. Noise Reduction

b. Artifact Removal

c. Geometric Reprojection

d. Contrast Enhancement/stretching

e. Edge Detection

f. Smoothing

g. Pattern Recognition

h. Other: _____

B. Spatial- vs. Gray scale Resolution

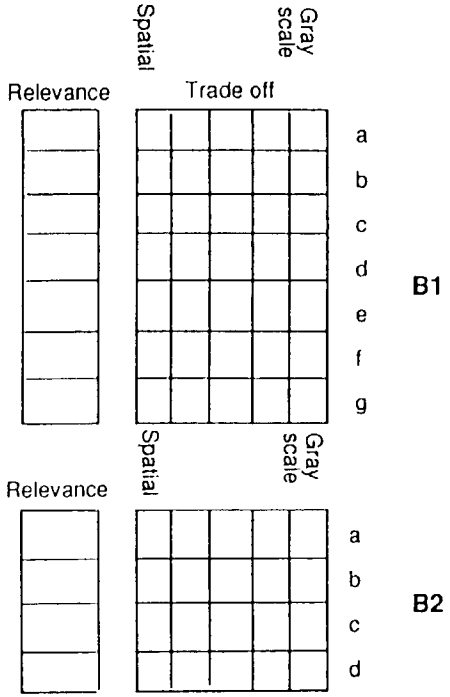

Team Memeber Name: _____

Form completed by (list): _____

_____

Institution _____

Tel.: _____

email: _____

SSI Experiment Questionaire Yaron Gold, 1993

Galileo SSI Team Survey Instructions (cont.)

B. Spatial - vs. Gray Scale Resolution

Use - Matrix **B1** and **B2** and the column labled "**Relevance.** Image compression based on the *Integer Cosine Transform* (ICT) dictates (and allows) a trade-off between spatial resolution and gray scale resolution for a given compression ratio, as explained and illustrated in Figure 2. We would like to have your opinion of how this trade-off impacts your own imaging requirements. To do this use matrices B1 and B2 (right side of form). The five cells in each row of these matrices allow you to indicate your relative preference for spatial - or gray scale resolution.

Specific Directions For Spatial- vs. Gray-Scale Resolution

- (B) For each **Application** you circled in Group **I - Visual Information Extraction** insert a numeric score between 1 and 10 in the column named "relevance". This number indicates your opinion regarding the significance of this trade off to the application (10 = most significant). All of the numbers within the relevance column must be unique, but need not be consecutive (for example, if you believe the tradeoff is highly and equally significant , for applications (b), (f) and (g), decide on some ranking order, and insert 10, 9 and 8 in the order you decided upon. If you believe that, say, (e) and (f) are moderately and equally significant for that application, and (b) is highly significant, insert 10 for (b), and 5 and 6 for the other two, after you decided on an order).

- (B') To indicate your trade off preference between spatial resolution versus gray scale resolution for a given application (only refer to those applications you rated in step B above), insert an "X" in the appropriate intermediate box. For example, an "X" placed closer to "Spatial" indicates that spatial resolution is more important to you for the given application than is gray scale resolution.

- (B") Repeat steps (B) and (B') for Application Group **II - Photometric Operations.** Use Matrix **B2.**

- *This concludes this survey. Thank you very much for your assistance* -

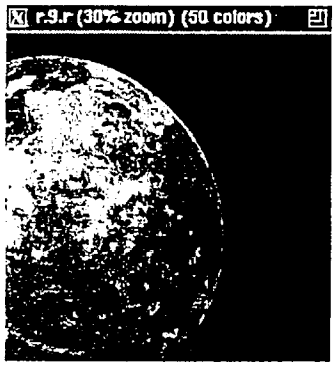

Solid with Limb

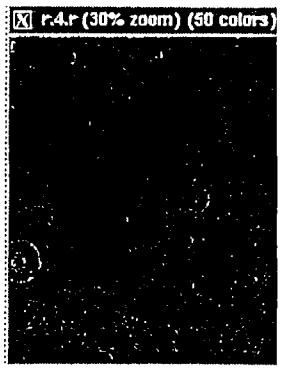

Solid without Limb

(Sattelites)

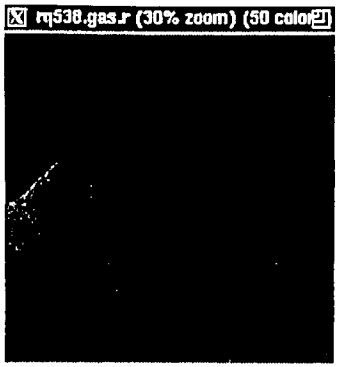

Small Bodies (eg: Asteroid)

(Most of image is dark sky)

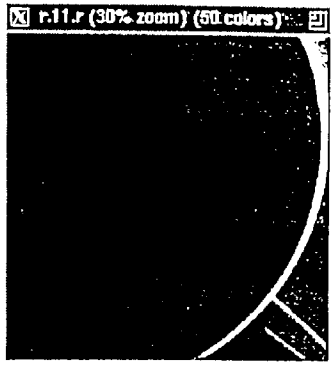

Rings

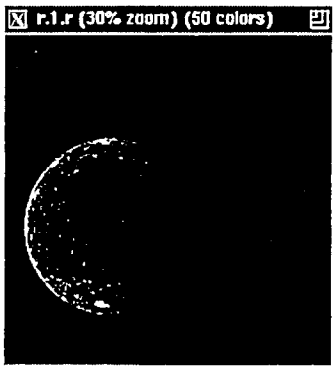

Solid with Terminator

(Not the best example, but you get the idea)

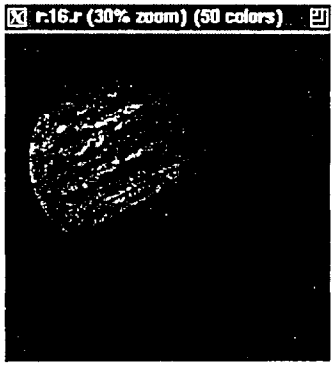

Gas with Limb

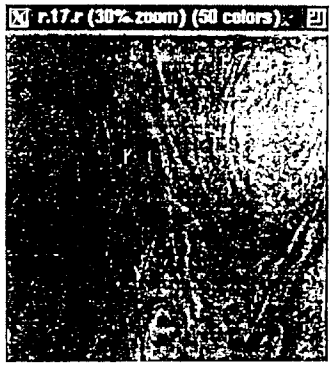

Gas without Limb

(i.e. Jupiter)

No Compression

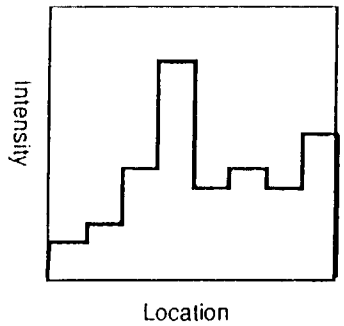

The Figures show intensity vs. location in a single dimension, across 8 pixels. This is a cross section through one 8x8 pixel block, which is the image unit for ict compression.

Low Gray-Scale Resolution

High Spatial Resolution

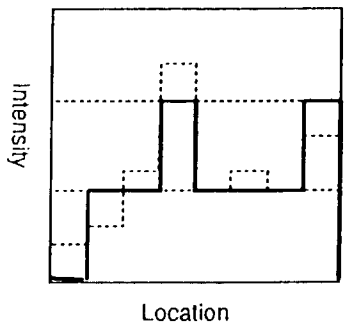

Small intensity peak is lost due to quantization;

Width and location of pronounced intensity peaks are preserved;

Difference in intensity between peaks is not preserved;

Allows precise localization, but not reliable photometric measurments.

High Gray-Scale Resolution

Low Spatial Resolution

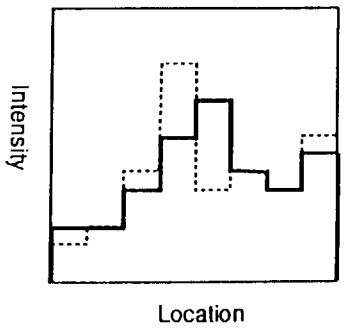

Average intensity in each 8x8 pixel block is preserved;

Difference in intensity between peaks is partially preserved;

Peaks "smeared" so –
small peak diffuses into its neighbors;
peak widths and locations are not preserved;

Allows precise photometric measurements, unless localized in a very small area.

Figure 2

Spatial– vs. Gray Scale Resolution

D. Pretest SSI Member Survey Results.

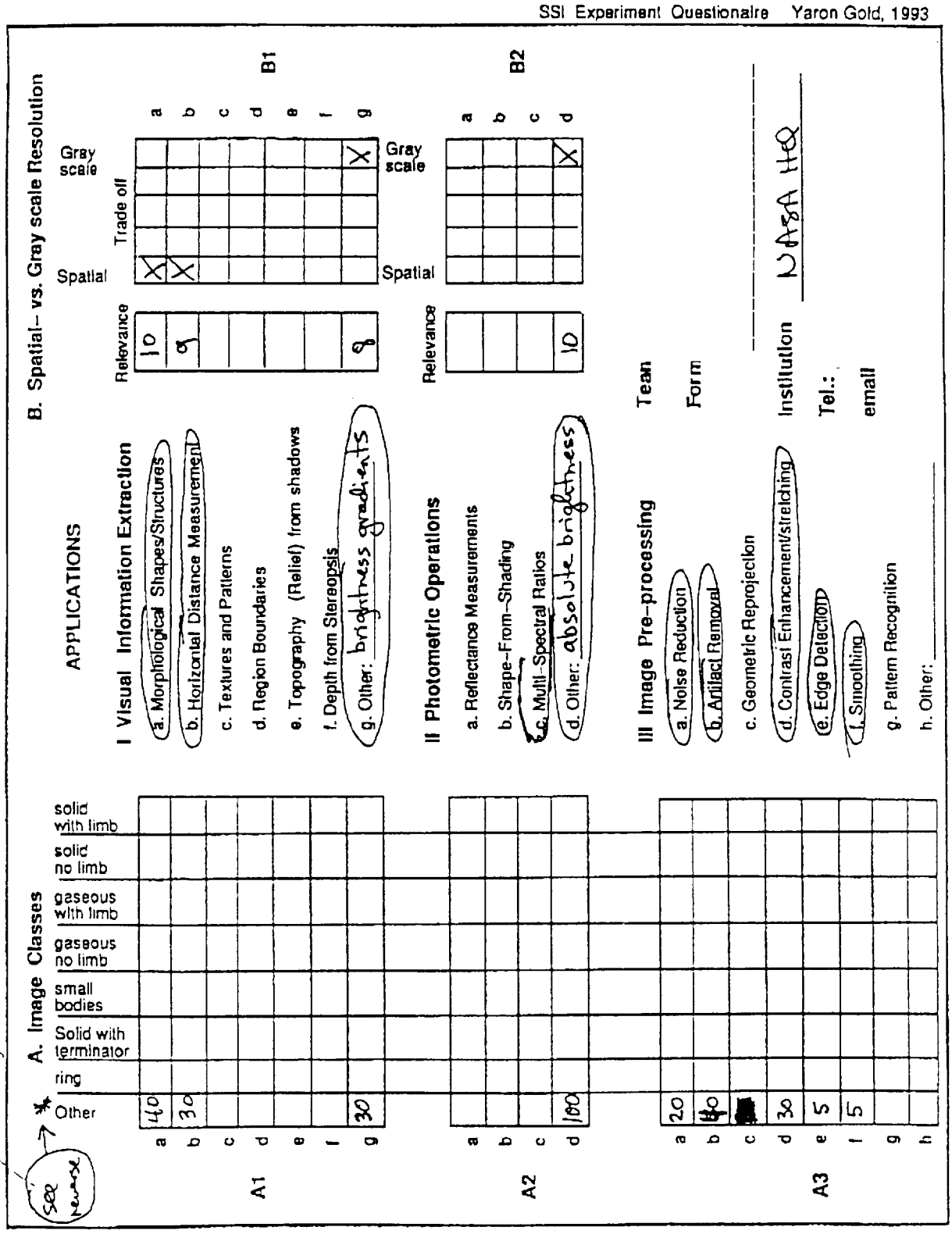

A. Image Classes

		Other	ring	Solid with terminator	small bodies	gaseous no limb	gaseous with limb	solid no limb	solid with limb
	a			25				25	25
	b			25				25	25
	c			10				20	20
A1	d			Ø				10	10
	e			20				Ø	Ø
	f			20				20	20
	g								
	a								
	b			80			70		Ø
A2	c			20			30		100
	d								
	a			5			5	5	
	b			5			5	5	
	c			30			30	30	
	d			30			30	30	
A3	e			30			30	30	
	f								
	g								
	h								

APPLICATIONS

I Visual Information Extraction

- (a.) Morphological Shapes/Structures
- (b) Horizontal Distance Measurement
- (c.) Textures and Patterns
- (d.) Region Boundaries
- (e.) Topography (Relief) from shadows
- (f.) Depth from Stereopsis
- g. Other: _____

II Photometric Operations

- a. Reflectance Measurements
- (b) Shape-From-Shading
- (c.) Multi-Spectral Ratios
- d. Other: _____

III Image Pre-processing

- (a) Noise Reduction
- (b) Artifact Removal
- (c) Geometric Reprojection
- (d.) Contrast Enhancement/stretching
- (e.) Edge Detection
- f. Smoothing
- g. Pattern Recognition
- h. Other: _____

B. Spatial- vs. Gray scale Resolution

B1

	Relevance	Spatial	Trade off			Gray scale	
a	10		X				a
b	9	X					b
c	7		X				c
d	5			X			d
e	6	X					e
f	8	X					f
g							g

B2

	Relevance	Spatial				Gray scale	
a							a
b	10					X	b
c	9					X	c
d							d

Team

Form

Institution NASA Ames

Tel.:

email:

A. Image Classes

		Other	ring	Solid with terminator	small bodies	gaseous no limb	gaseous with limb	solid no limb	solid with limb
(716)	a	50	25	25	33	33	25	25
165	b		25	25	33	33	25	25
	c								
185	A1 d	50	25	25	34	34	25	25
100	e		25	25			25	25
	f								
	g	100							
(210)	a	50	33	33	33	33	33	33
135	b		33	33			33	33
	A2 c	50	34	34	33	33	34	34
(210)									
100	d	100							
	a		25	16	16	16	16	16	16
	b		25	16	16	17	16	16	16
	c			16	16	17	16	16	16
	d		25	17	17	16	17	17	17
	A3 e			17	17		17		17
	f		25	16	16	17	17	17	17
	g								
	h								

YES

APPLICATIONS

I Visual Information Extraction

- (a) Morphological Shapes/Structures
- (b) Horizontal Distance Measurement
- c. Textures and Patterns
- (d) Region Boundaries
- (e) Topography (Relief) from shadows
- f. Depth from Stereopsis
- g. Other: DARK SIDE - LIGHTNING + AURORAE

II Photometric Operations

- (a) Reflectance Measurements
- (b) Shape-From-Shading
- (c) Multi-Spectral Ratios
- d. Other: DARK SIDE - LIGHTNING - AURORAE

III Image Pre-processing

- (a) Noise Reduction
- (b) Artifact Removal
- (c) Geometric Reprojection
- (d) Contrast Enhancement/stretching
- (e) Edge Detection
- (f) Smoothing
- g. Pattern Recognition
- h. Other: _____

B. Spatial- vs. Gray scale Resolution

	Relevance	Spatial			Gray scale	
B1	10	X				a
	8	X				b
	9				X	c
	7		X		X	d
	6					e
						f
						g

	Relevance	Spatial			Gray scale	
B2	10				X	a
	8		X			b
	9				X	c
	7		X			d

Team

Form

Institution NOAO

Tel.:

email:

A. Image Classes

		Other	ring	Solid with terminator	small bodies	gaseous no limb	gaseous with limb	solid no limb	solid with limb
30	a					15	15		
100	b					50	50		
30	c					15	15		
35 A1	d					15	20		
5	e					5			
	f								
	g								
40	a					20	20		
20	b					10	10		
A2 140	c					70	70		
	d								
	a					50	50		
	b					50	50		
	c								
	d								
A3	e								
	f								
	g								
	h								

YES

APPLICATIONS

I Visual Information Extraction

- a. Morphological Shapes/Structures
- b. Horizontal Distance Measurement
- c. Textures and Patterns
- d. Region Boundaries
- e. Topography (Relief) from shadows
- f. Depth from Stereopsis
- g. Other: _____

II Photometric Operations

- a. Reflectance Measurements
- b. Shape-From-Shading
- c. Multi-Spectral Ratios
- d. Other: _____

III Image Pre-processing

- a. Noise Reduction
- b. Artifact Removal
- c. Geometric Reprojection
- d. Contrast Enhancement/stretching
- e. Edge Detection
- f. Smoothing
- g. Pattern Recognition
- h. Other: _____

B. Spatial- vs. Gray scale Resolution

B1

	Relevance	Spatial	Gray scale
a	8	X	
b	10	X	
c	7	X	
d	9	X	
e	6	X	
f			
g			

B2

	Relevance	Spatial	Gray scale
a	5		X
b	4	X	
c	6		X
d			

Team

Form

Institution Caltech (170-25)

Tel.:

email:

or

A. Image Classes

			Other	ring	Solid with terminator	small bodies	gaseous no limb	gaseous with limb	solid no limb	solid with limb
120	a				30	50			25	20
60	b				10	10			25	20
105	c				30	20			25	30
35	A1	d			30	20			25	30
		e								
		f								
		g								
160		a		33	30	33			40	30
		b								
64	A2	c		33	30	33			40	30
160		d		33	40	33			20	40
110		a		15	15	20	15	15	15	15
110		b		15	15	20	15	15	15	15
90		c		15	15		15	15	15	15
110		d		15	15	20	15	15	15	15
	A3	e		10	10	20	10	10	10	10
30		f		5	5		5	5	5	5
		g								
170		h		25	25	20	25	25	25	25

APPLICATIONS

I Visual Information Extraction

- (a) Morphological Shapes/Structures
- (b) Horizontal Distance Measurement
- (c) Textures and Patterns
- (d) Region Boundaries
- e. Topography (Relief) from shadows
- f. Depth from Stereopsis
- g. Other: _____

II Photometric Operations

- (a) Reflectance Measurements
- b. Shape-From-Shading
- (c) Multi-Spectral Ratios
- (d) Other: PHASE FUNCTION DETERMINATION (brightness variation as function of phase angle)

III Image Pre-processing

- (a) Noise Reduction
- (b) Artifact Removal
- (c) Geometric Reprojection
- (d) Contrast Enhancement/stretching
- (e) Edge Detection SHARPENING
- (f) Smoothing
- g. Pattern Recognition
- (h) Other: clustering/classification

B. Spatial- vs. Gray scale Resolution

Relevance	Spatial	Gray scale				
8	X					a
7	X					b
9	X					c
10					X	d
						e
						f
						g

B1

Relevance	Spatial	Gray scale				
10					X	a
						b
8					X	c
9					X	d

B2

Tear

Form

Institution LPL, Univ. Arizona

Tel.:

email

SSI Experiment Questionnaire Yaron Gold, 1993

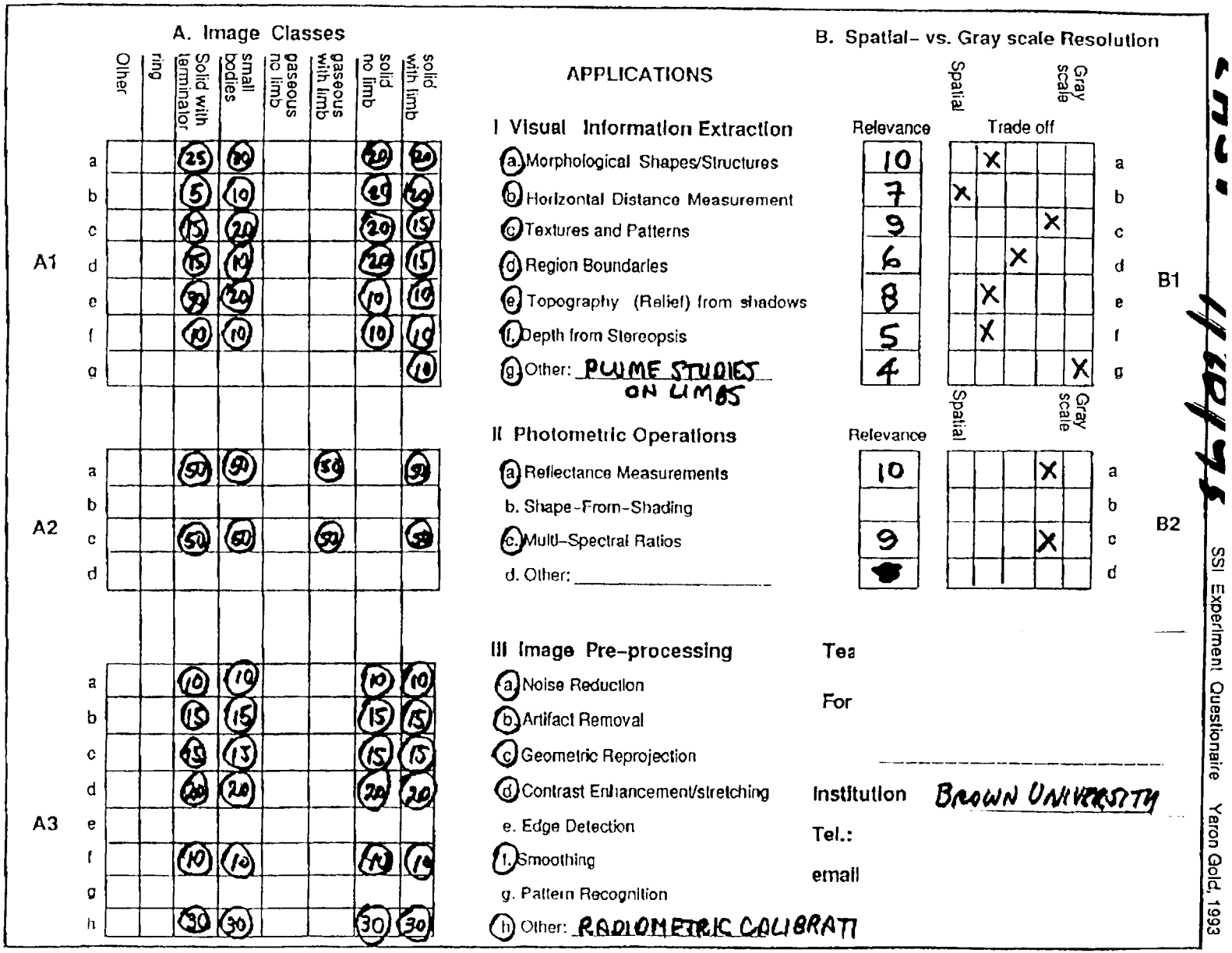

SSI Experiment Questionnaire Yaron Gold, 1993

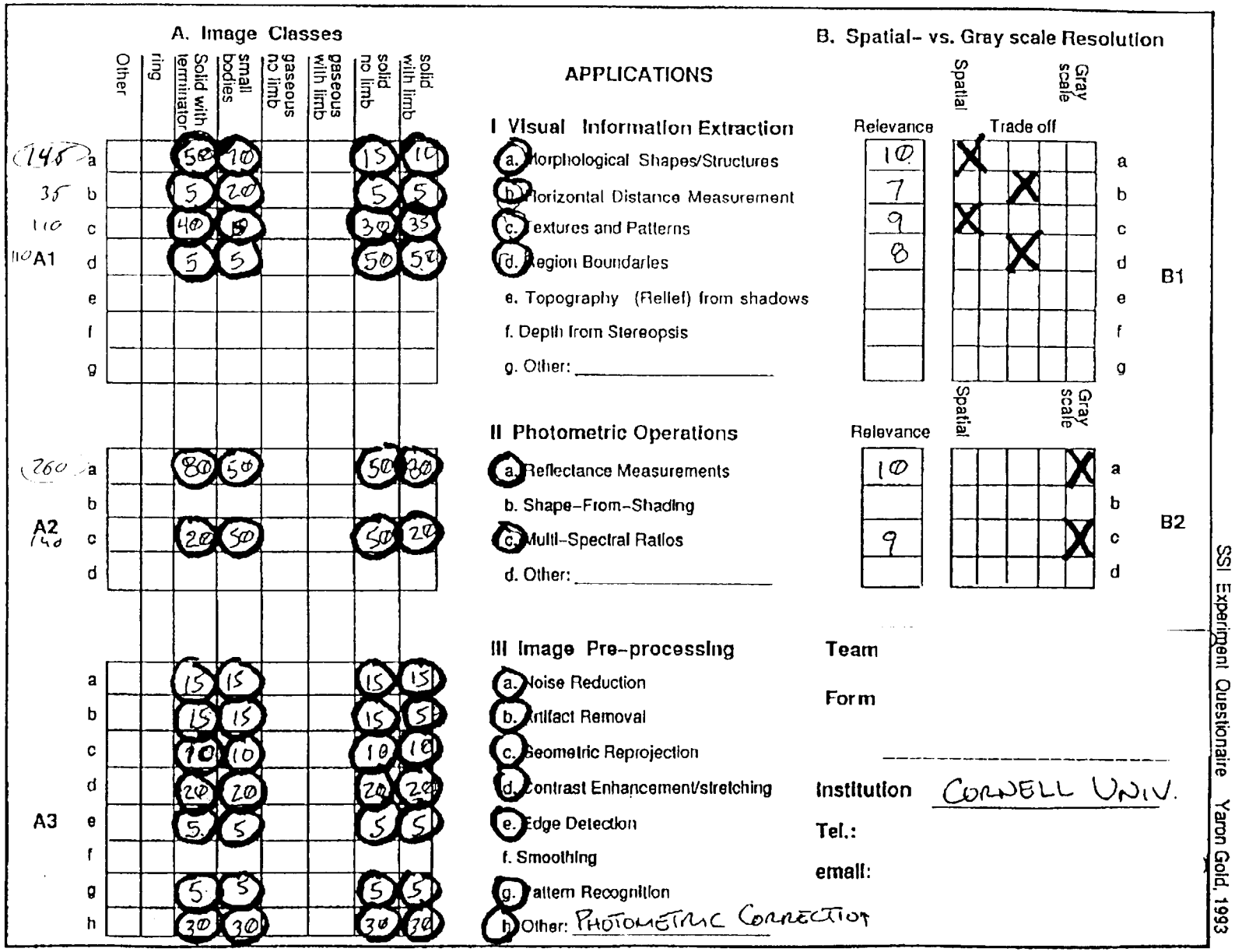
A. Image Classes
Other
ring
Solid with terminator
small bodies
gaseous no limb
gaseous with limb
solid no limb
solid with limb
(148) a 50 10 15 10
35 b 5 20 5 5
110 c 40 50 30 35
110 A1 d 5 5 50 50
e
f
g
(260) a 80 50 50 80
b
A2 (140) c 20 50 50 20
d
a 15 15 15 15
b 15 15 15 5
c 10 10 10 10
d 20 20 20 20
A3 e 5 5 5 5
f
g 5 5 5 5
h 30 30 30 30
APPLICATIONS
I Visual Information Extraction
a. Morphological Shapes/Structures
b. Horizontal Distance Measurement
c. Textures and Patterns
d. Region Boundaries
e. Topography (Relief) from shadows
f. Depth from Stereopsis
g. Other: _____
II Photometric Operations
a. Reflectance Measurements
b. Shape-From-Shading
c. Multi-Spectral Ratios
d. Other: _____
III Image Pre-processing
a. Noise Reduction
b. Artifact Removal
c. Geometric Reprojection
d. Contrast Enhancement/stretching
e. Edge Detection
f. Smoothing
g. Pattern Recognition
h. Other: PHOTOMETRIC CORRECTION
B. Spatial- vs. Gray scale Resolution
Spatial
Gray scale
Relevance
Trade off
10 a
7 b
9 c
8 d
e
f
g
B1
Spatial
Gray scale
Relevance
10 a
b
9 c
d
B2
Team
Form
Institution CORNELL UNIV.
Tel.:
email:

YES

13

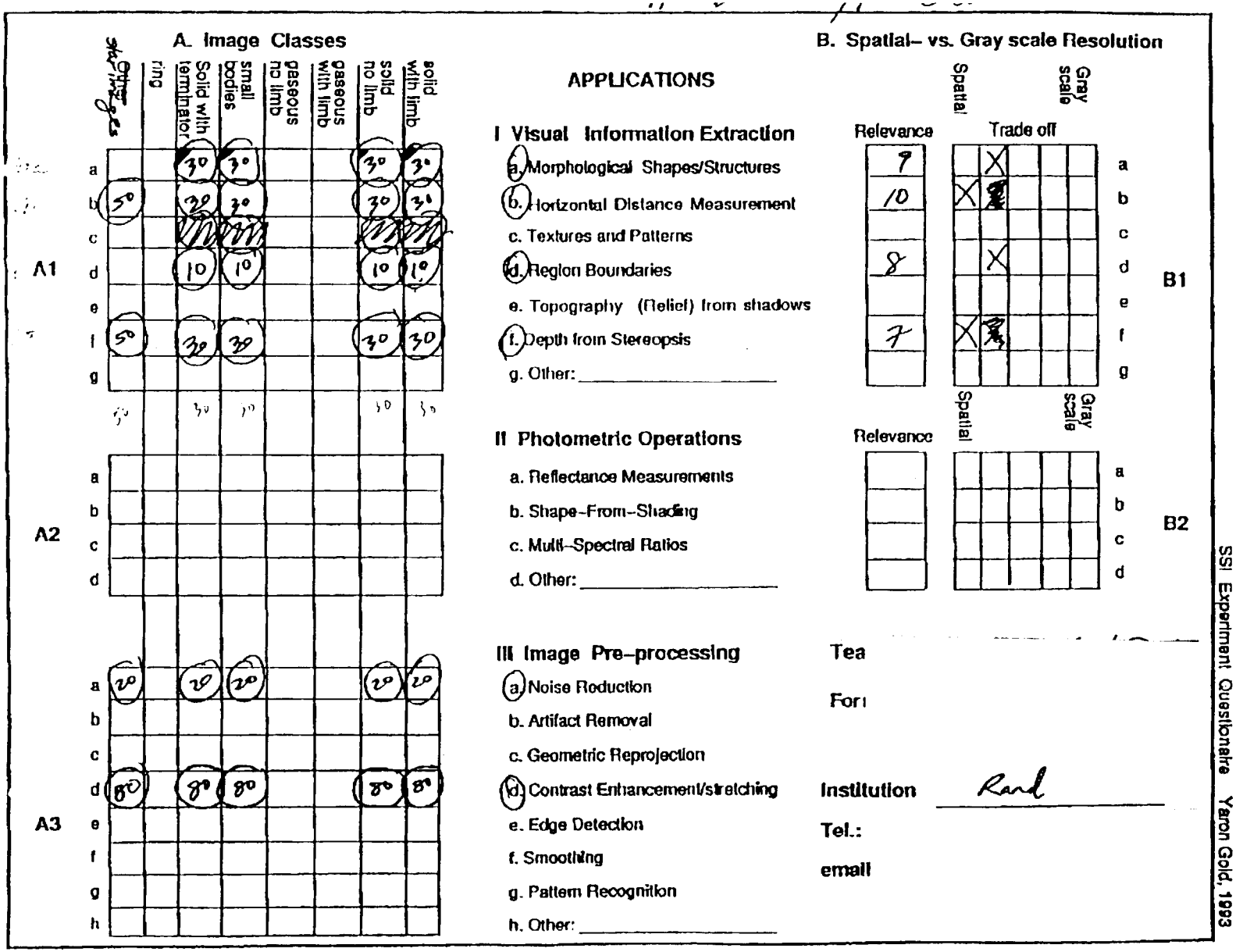

SSI Experiment Questionaire Yaron Gold, 1993

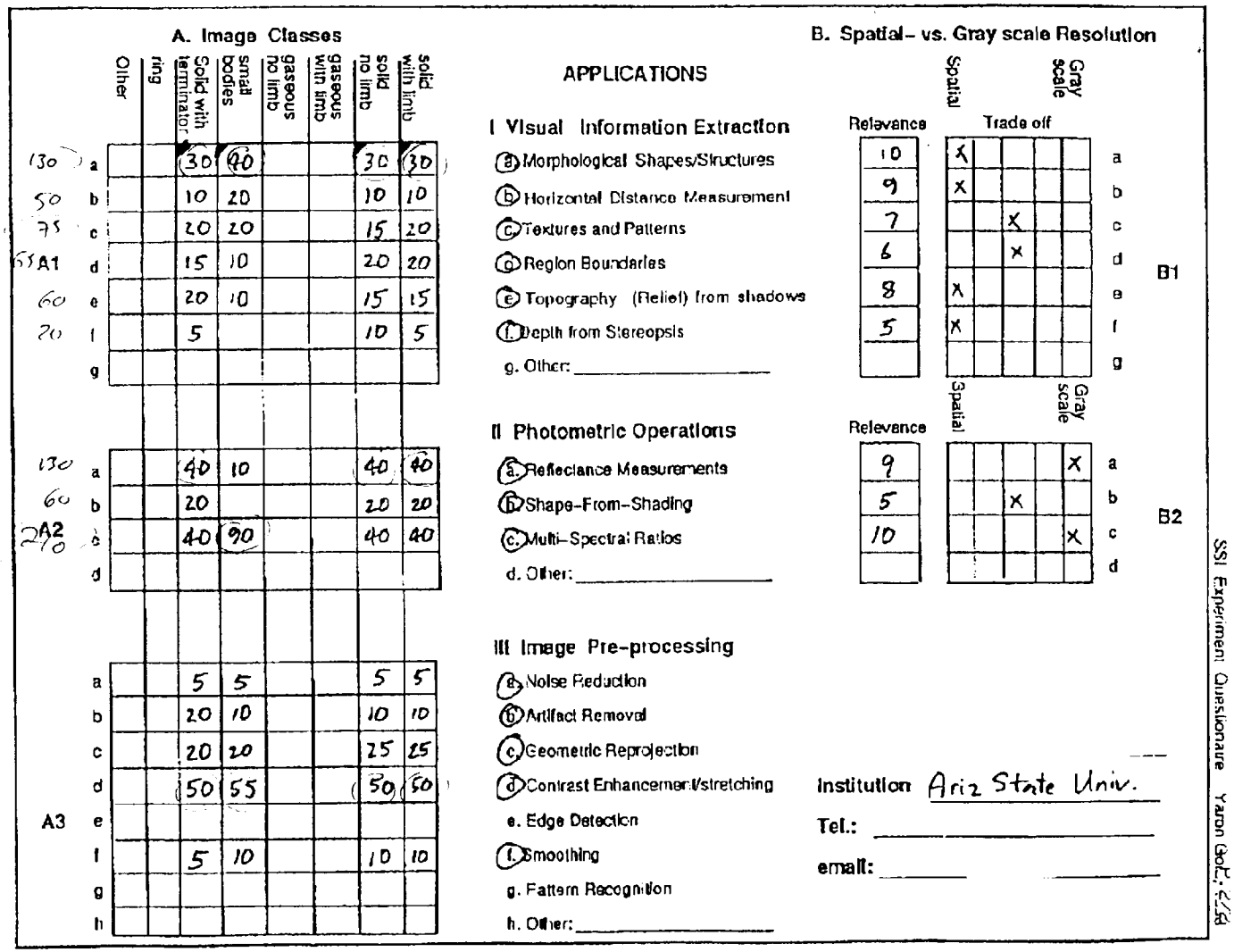

SSI Experiment Questionnaire Yaron Gold: 4/88

A. Image Classes

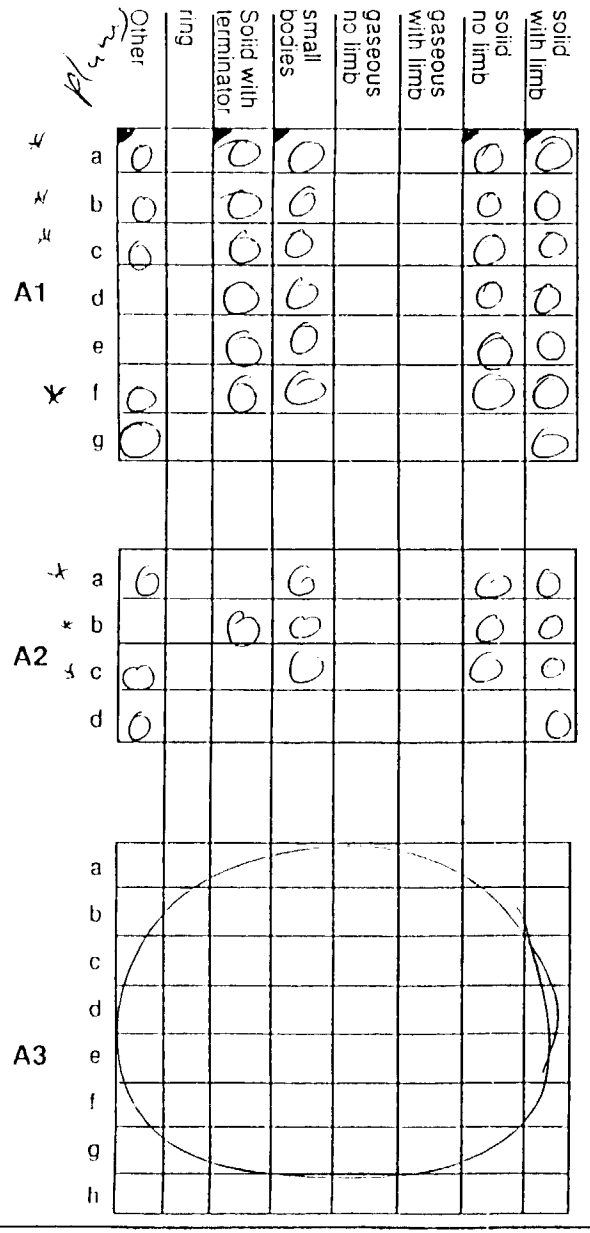

APPLICATIONS

I Visual Information Extraction

- (a.) Morphological Shapes/Structures
- (b.) Horizontal Distance Measurement
- (c.) Textures and Patterns
- (d.) Region Boundaries
- (e.) Topography (Relief) from shadows
- (f.) Depth from Stereopsis
- (g.) Other: To planes stereoscopy

II Photometric Operations

- (a.) Reflectance Measurements
- (b.) Shape-From-Shading
- (c.) Multi-Spectral Ratios
- (d.) Other: 3 planes photometry

III Image Pre-processing

- (a.) Noise Reduction
- (b.) Artifact Removal
- (c.) Geometric Reprojection
- (d.) Contrast Enhancement/stretching
- (e.) Edge Detection
- (f.) Smoothing
- (g.) Pattern Recognition
- (h.) Other: radiometric calibration

B. Spatial- vs. Gray scale Resolution

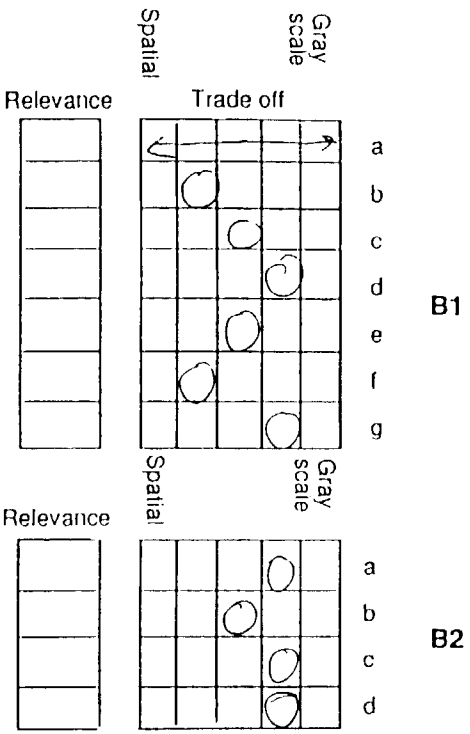

Team A

Form c

Institution USGS

Tel.:

email:

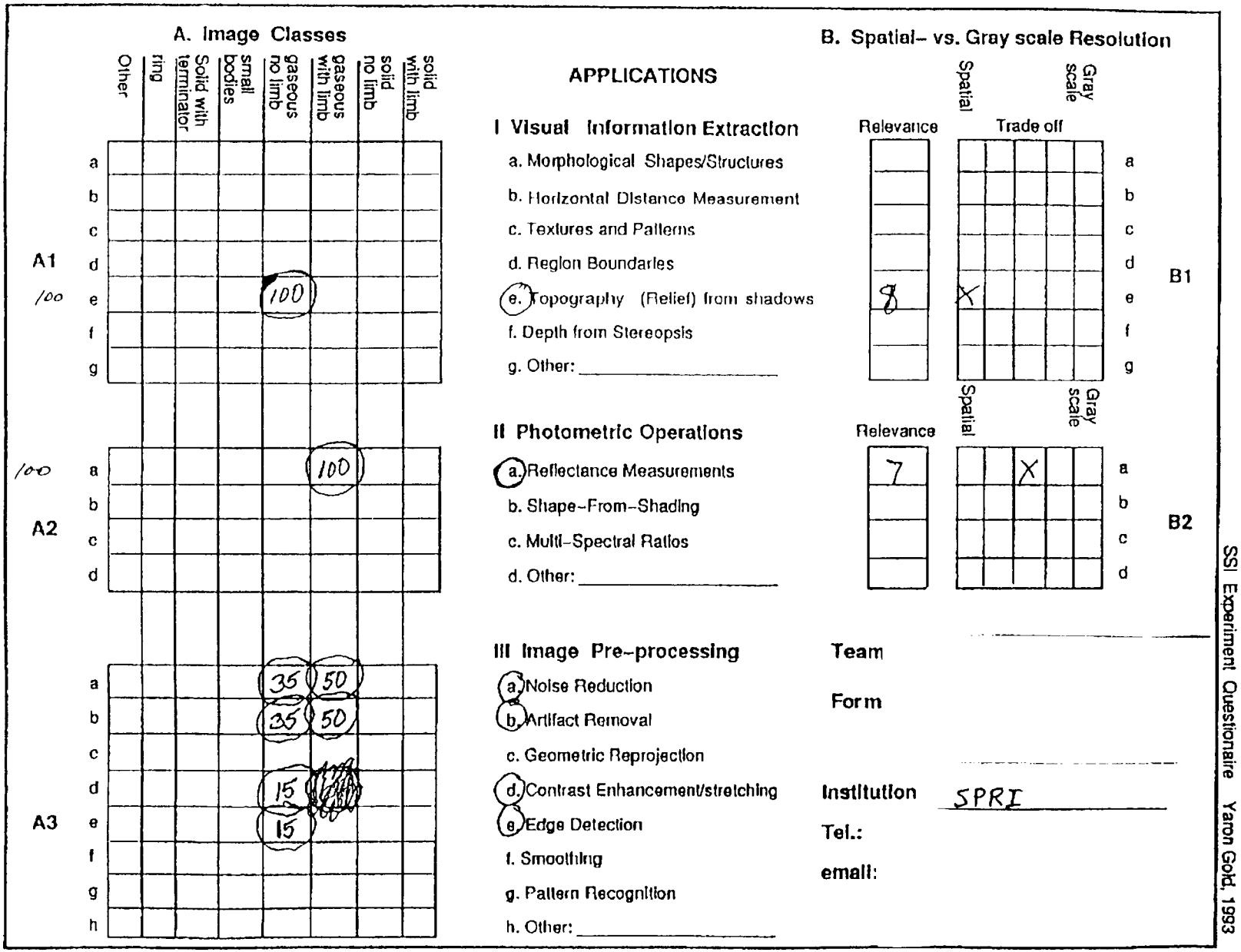
A. Image Classes
Other
ring
Solid with terminator
small bodies
gaseous no limb
gaseous with limb
solid no limb
solid with limb
A1
A2
A3
100
100
35
50
25
50
15
15
APPLICATIONS
I Visual Information Extraction
a. Morphological Shapes/Structures
b. Horizontal Distance Measurement
c. Textures and Patterns
d. Region Boundaries
e. Topography (Relief) from shadows
f. Depth from Stereopsis
g. Other:
II Photometric Operations
a. Reflectance Measurements
b. Shape-From-Shading
c. Multi-Spectral Ratios
d. Other:
III Image Pre-processing
a. Noise Reduction
b. Artifact Removal
c. Geometric Reprojection
d. Contrast Enhancement/stretching
e. Edge Detection
f. Smoothing
g. Pattern Recognition
h. Other:
B. Spatial- vs. Gray scale Resolution
Spatial
Gray scale
Relevance
Trade off
B1
B2
Team
Form
Institution SPRI
Tel.:
email:
SSI Experiment Questionaire Yaron Gold, 1993

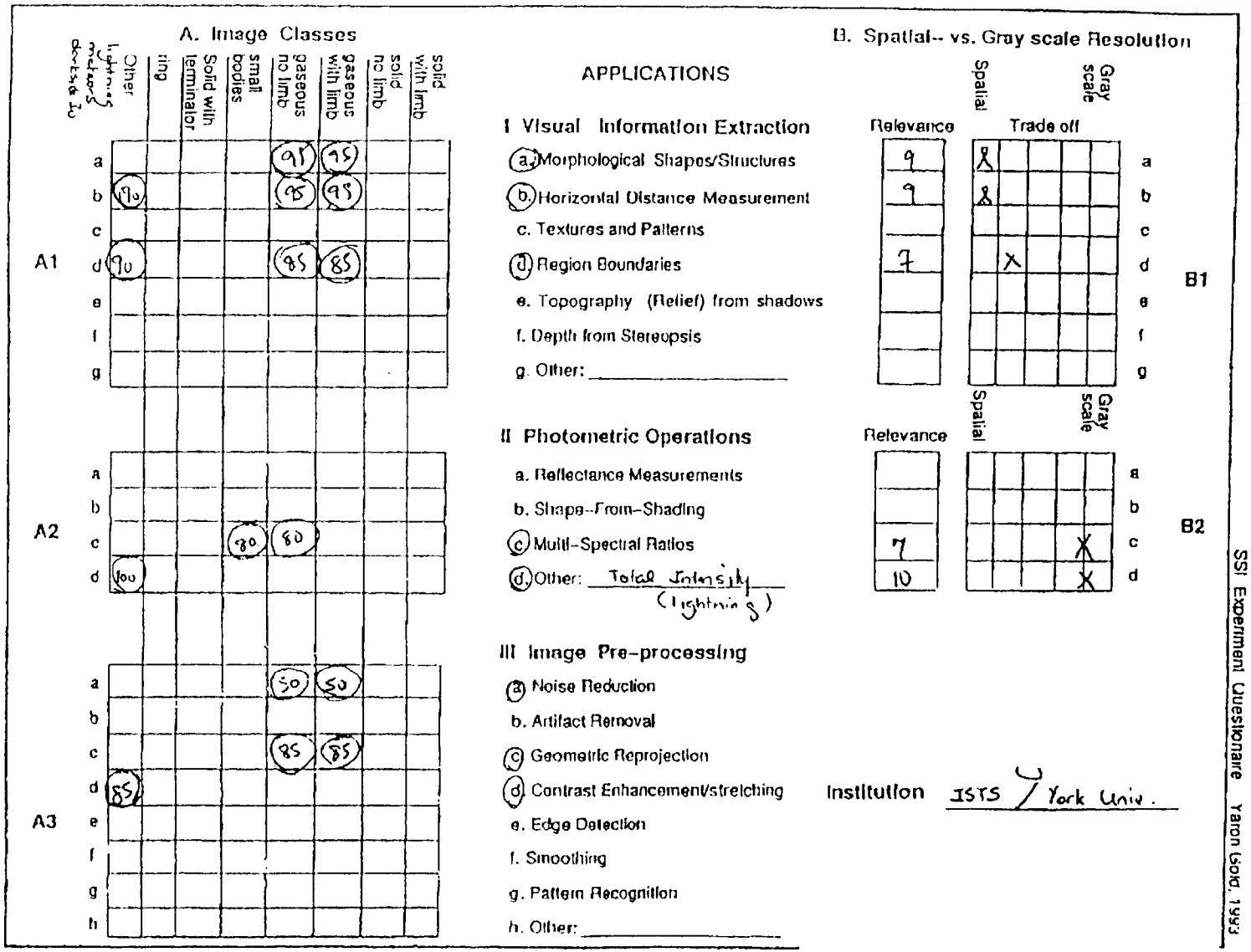
A. Image Classes
Other lightning sources
ting
Solid with terminator
small bodies
gaseous no limb
gaseous with limb
solid no limb
solid with limb
A1
A2
A3
APPLICATIONS
I Visual Information Extraction
a. Morphological Shapes/Structures
b. Horizontal Distance Measurement
c. Textures and Patterns
d. Region Boundaries
e. Topography (Relief) from shadows
f. Depth from Stereopsis
g. Other:
II Photometric Operations
a. Reflectance Measurements
b. Shape-From-Shading
c. Multi-Spectral Ratios
d. Other: Total Intensity (lightning)
III Image Pre-processing
a. Noise Reduction
b. Artifact Removal
c. Geometric Reprojection
d. Contrast Enhancement/stretching
e. Edge Detection
f. Smoothing
g. Pattern Recognition
h. Other:
B. Spatial-- vs. Gray scale Resolution
Spatial
Gray scale
Relevance
Trade off
B1
B2
Institution ISTS / York Univ.

A. Image Classes

		Other	ring	Solid with terminator	small bodies	gaseous no limb	gaseous with limb	solid no limb	solid with limb
A1	a								
	b								
	c								
	d								
	e								
	f								
	g								
A2	a		35	30	30	35	35	30	30
	b			10	20			10	10
	c		35	30	30	35	35	30	30
	d	60							
A3	a	20	15	15	10	15	15	15	15
	b	20	15	15	10	15	15	15	15
	c								
	d								
	e								
	f								
	g								
	h								

APPLICATIONS

I Visual Information Extraction

a. Morphological Shapes/Structures
b. Horizontal Distance Measurement
c. Textures and Patterns
d. Region Boundaries
e. Topography (Relief) from shadows
f. Depth from Stereopsis
g. Other: _____

II Photometric Operations

(a.) Reflectance Measurements
(b.) Shape-From-Shading
(c.) Multi-Spectral Ratios
(d.) Other: INSTRUMENT CALIBRATION

III Image Pre-processing

(a.) Noise Reduction
(b.) Artifact Removal
c. Geometric Reprojection
d. Contrast Enhancement/stretching
e. Edge Detection
f. Smoothing
g. Pattern Recognition
h. Other: _____

B. Spatial- vs. Gray scale Resolution

B1

	Relevance	Spatial	Gray scale
a			
b			
c			
d			
e			
f			
g			

B2

	Relevance	Spatial	Gray scale
a	7		X
b	6	X	
c	8	X	
d	5	X	

Team

Form

Institution JPL

Tel.:

email:

SSI Experiment Questionaire Yau & Gold, 1993

E. Test Instructions

Instructions

Note to Experimenter
It is very important for you to read these instructions out loud to every subject in the same way. Try to not emphasize a part of them to one subject differently than to another subject.

The experiment in which you are about to take part is designed to find out the impact which various digital image compression parameters have on the usefulness and acceptability of Galileo-type images to you. As has been mentioned already, we will present two different digitized images to you. Each will be compressed and decompressed using the ICT (Integer Cosine Transform) algorithm with specially developed Q tables. We will also present a number of compression levels for each image and Q table. In addition, the images also may include noise which has been compressed and decompressed prior to display.

Most of these images have been enlarged 200% in order to better illustrate pixel-level compression effects to you. In addition, they have been cropped in order to fit two images side by side on the display to allow you to make simultaneous visual comparisons of their quality. *Here is what you are to do.*

First sit comfortably with your eyes located about 18 - 20" from and normal to the screen. If you wear reading or image viewing glasses put them on.

Second. For familiarization purposes you will be shown one uncompressed and a second highly compressed image side by side. It should be obvious which is which. Compare their features carefully. Try to use the same judgment criteria when evaluating*all* of the following images, i.e., don't change your subjective acceptance criteria during the test.

Third. After the experimenter brings up the first pair of test images on the screen you are to examine them (we recommend about 20 seconds) and then select the image which you think is of the highest overall quality to support you in doing your work.

"Tell the experimenter "left" or "right" to indicate which image it was."

Fourth. Using a rating scale from 1 to 5 give a numeric value to each images. The experimenter will record them.

	- Key -
"Tell the experimenter the number you would use to best describe the image's scientific usefulness or value to you (as you study/quantify /use that image.)"	**1 = totally useless (without any scientific merit)** **3 = about average usefulness/value or merit** **5 = highest possible usefulness/value or merit**

The next pair of images will be presented immediately. Simply repeat the above steps for each pair of images. Please understand that we cannot tell you anything about the nature of the compression or Q tables being used or other technical details until the data collection is completed. This will ensure a more unbiased comparison of the variables and make it possible to extrapolate the statistical findings to a larger number of scientists.

F. Table of Actual Voyager Data and Simulated Galileo

Data File Parameters

	ACTUAL VOYAGER DATA						SIMULATED GALILEO DATA			
FILE	TARGET	CRAFT	CAMERA	RATE	FILTER	EXP(MS)	FILTER	GAIN	RATE	EXP(MS)
R.1	CALLISTO	1	NA	1	CLEAR	480	RED	100K	60.67	8.33
R.2	CALLISTO	1	NA	1	VIOLET	1920	RED	100K	60.67	8.33
R.3	GANYMEDE	2	NA	1	CLEAR	180	RED	100K	60.67	8.33
R.4	GANYMEDE	2	NA	1	CLEAR	120	RED	100K	60.67	8.33
R.5	EUROPA	2	NA	1	CLEAR	120	RED	100K	60.67	8.33
R.6	EUROPA	2	NA	1	ORANGE	480	RED	100K	60.67	8.33
R.7	IO	1	NA	1	CLEAR	360	RED	100K	60.67	8.33
R.8	IO	1	NA	1	CLEAR	360	RED	100K	60.67	8.33
R.9	IO	1	NA	1	CLEAR	180	RED	100K	60.67	8.33
R.10	AMALTHEA	1	NA	1	CLEAR	2880	RED	100K	60.67	8.33
R.11	RING	2	WA	1	ORANGE	96000	RED	100K	60.67	8.33
R.12	JUP	1	WA	1	ORANGE	360	8890	100K	60.67	133.33
R.13	JUP	1	NA	1	ORANGE	960	8890	100K	60.67	133.33
R.14	JUP	2	NA	1	ORANGE	720	8890	100K	60.67	133.33
R.15	JUP	1	NA	1	ORANGE	960	8890	100K	60.67	133.33
R.16	JUP	1	WA	1	VIOLET	180	VIOL	100K	60.67	66.67
R.17	JUP	1	NA	1	VIOLET	480	VIOL	100K	60.67	66.67
R.18	JUP	2	NA	1	VIOLET	360	VIOL	100K	60.67	66.67
R.19	JUP	1	NA	1	VIOLET	480	VIOL	100K	60.67	66.67

G. SUN Monitor Pixel Dimensions (mm)

Color	Monitor 1	Monitor 2	Monitor 3
Single pixel (edge to edge)			
Red	0.048	0.048	0.048
Green	0.048	0.059	0.048
Blue	0.036	0.048	0.036
Inter-pixel distance (center to center)			
Green–red	0.178	0.190	0.178
Green–green	0.309	0.309	0.321
Green–blue	0.107	0.119	0.095

H. Remainder of Test Results

Solid surface with limb images–Figure H-1(a) (file r.9.r) represents the second example of a solid surface with limb, but no noise present. Unlike the previous example (r.6.r, fig. 6(a)), this surface is characterized by larger homogeneous surface areas with numerous compact crater-like forms. The acceptable safe ranges of ICT quantization (and corresponding compressions) for each of the three (figs. H-1(b)–(d)) q tables are significantly greater than are those for the previous example (fig. 6(b)–(d)). For q table 0, the image was acceptable with a compression ratio greater than 37:1. The compression range of q table 1 was a safe 35:1 to 46:1, and q table 2 was even higher. The transition in scores from positive to negative in figure H-1(b)–(d) was determined by evaluators 2 and 3 (neither was preselected to be a test participant and may or may not be particularly qualified to rate these images).

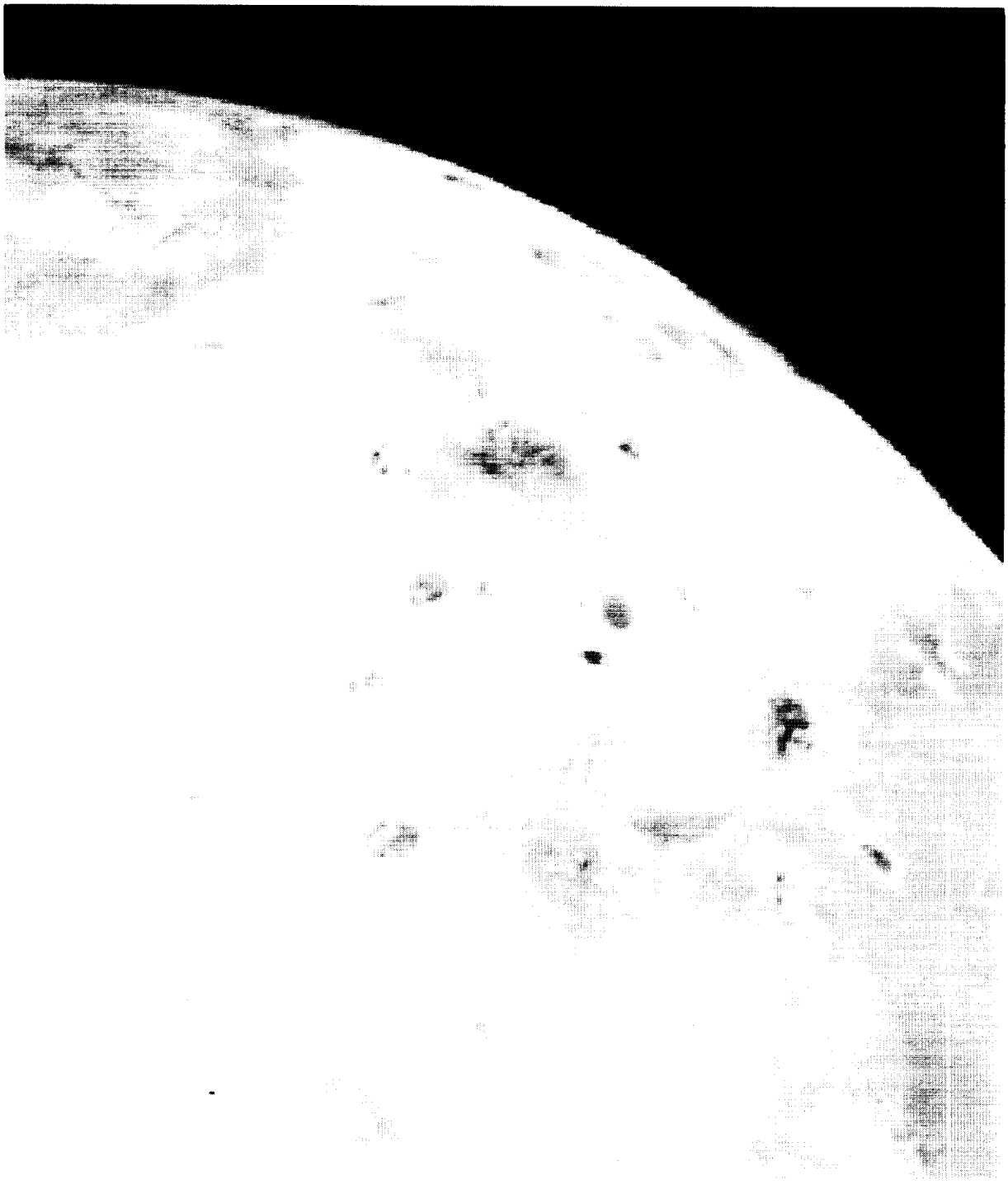

Figure H-1.(a) Image file r.9.r (Io) as presented to evaluators.

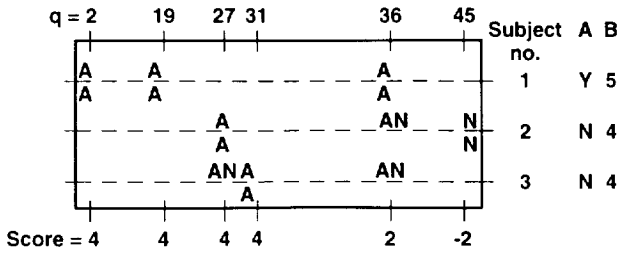

Safe range 36 - 45 Compression ratios 37 - 42
Likely range 36 - 45 Compression ratios 37 - 42

Figure H-1. (b) File r.9.r (lo) using q table 0.

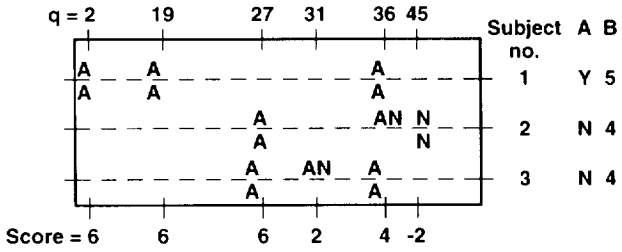

Safe range 27 - 45 Compression ratios 35 - 46
Likely range 36 - 45 Compression ratios 41 - 46

Figure H-1. (c) File r.9.r (lo) using q table 1.

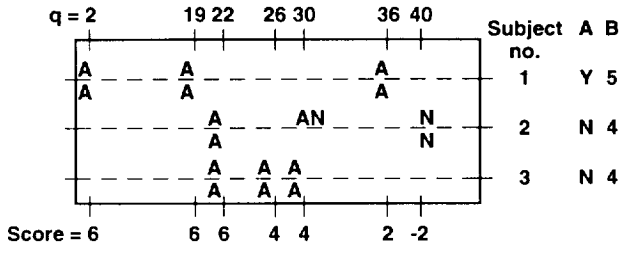

Safe range 36 - 40 Compression ratios 44 - 46
Likely range 36 - 40 Compression ratios 44 - 46

Figure H-1. (d) File r.9.r (lo) using q table 2.

Solid surface with limb plus noise– Figure H-2(a) makes it possible to directly compare the influence of one type of superimposed (type B) radiation noise upon the acceptable range of compression for each of the three q tables tested. For q table 0, acceptable compression ratios of only 1:1 to 5:1 are produced for the noisy image as compared with the no noise image (r.6.r, fig. 6(a)), which was judged as acceptable with compressions of 8:1 to 12:1. The q tables 1 and 2 yielded smaller differences between the noisy and no-noise images.

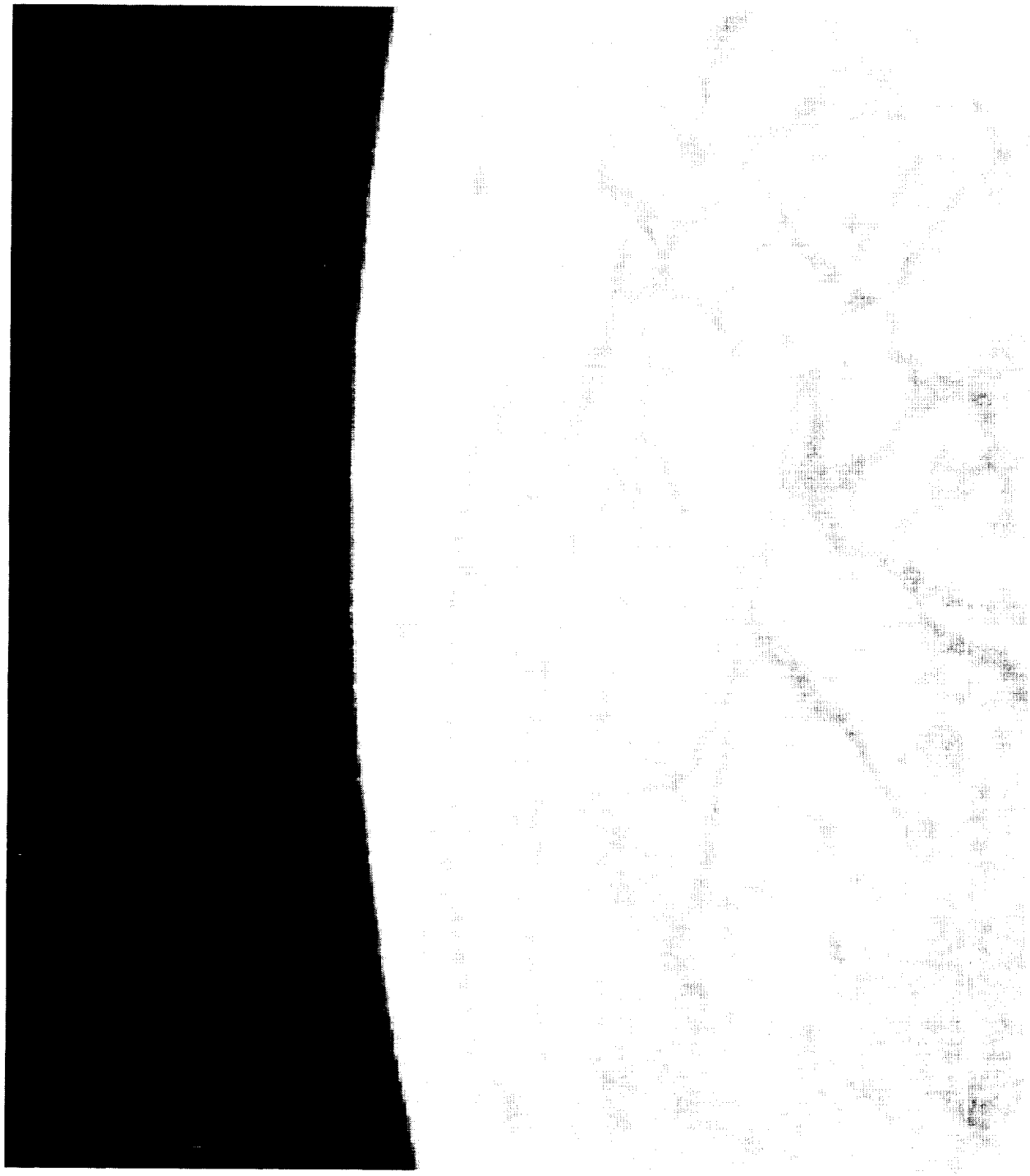

Figure H-2. (a) Image file r6.noise.r (Europa) as presented to evaluators.

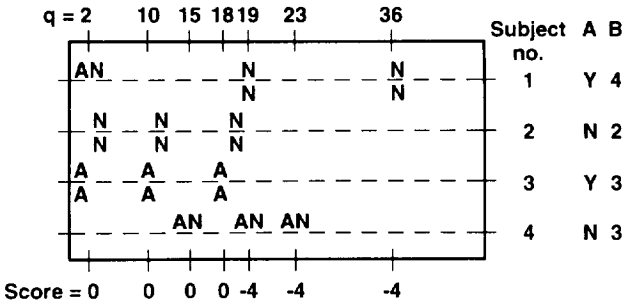

Safe range 2 - 19 Compression ratios 1 - 5
Likely range 15 - 19 Compression ratios 4 - 5

Figure H-2. (b) file r6.noise.r (Europa) using q table 0.

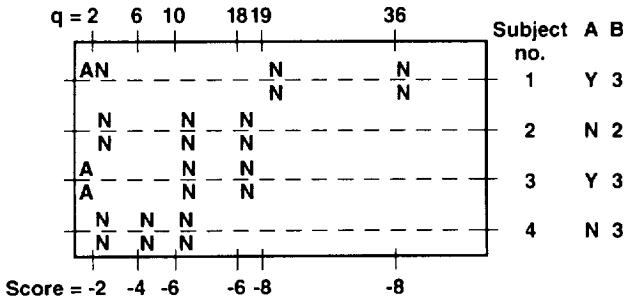

Safe range < 2 Compression ratios < 2
Likely range < 2 Compression ratios < 2

Figure H-2. (c) File r6.noise.r (Europa) using q table 1.

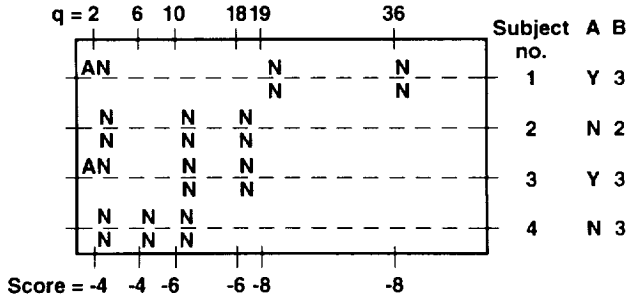

Safe range < 2 Compression ratios < 3
Likely range < 2 Compression ratios < 3

Figure H-2.(d) File r6.noise.r (Europa) using q table 2.

Solid surface without limb– Comparing the relatively high acceptable ICT compression ratio data found in figure H-3(b)–(d) (as high as 41:1 using q table 1) with the image being rated (fig. H-3(a)) suggests that there is a great deal of redundant information in this image. The redundant information may be in the broad, flat, homogeneous surfaces. Nevertheless, what is redundant and therefore a candidate for mathematical elimination or distortion from a compression standpoint may still be important from a visual evaluation standpoint. The smallest range of acceptable compressions was associated with q table 0.

Figure H-3. (a) Image file sr7.raw.r (Io) as presented to evaluators.

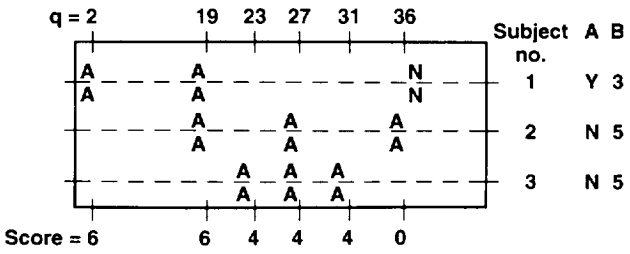

Safe range > 36 Compression ratios > 38
Likely range > 36 Compression ratios > 38

Figure H-3. (b) File sr7.raw.r (lo) using q table 0.

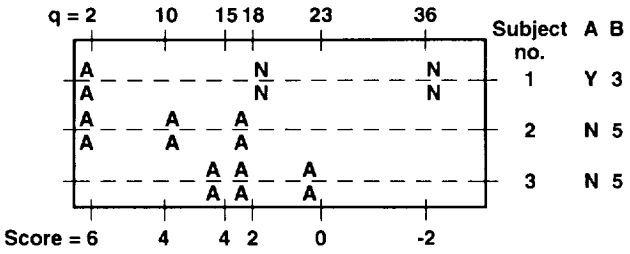

Safe range 18 - 36 Compression ratios 23 - 41
Likely range 18 - 36 Compression ratios 23 - 41

Figure H-3.(c) File sr7.raw.r (lo) using q table 1.

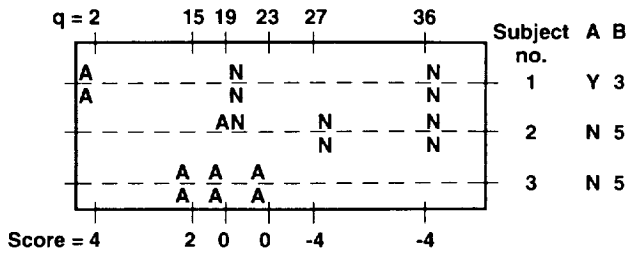

Safe range 15 - 27 Compression ratios 23 - 36
Likely range 15 - 27 Compression ratios 23 - 36

Figure H-3. (d) File sr7.raw.r (lo) using q table 2.

Solid surface without limb plus noise–The type C radiation noise used in figure H-4(a) consisted primarily of small compact clusters of 5 to 10 pixels each with several longer, linear, high-contrast streaks. A random array of such dots and lines was translated horizontally and down a distance of about 15 cluster diameters and then repeated. The acceptable range of ICT compression found for q table 0, 1, and 2 was from 4:1 to 8:1, <3:1, and <4:1, respectively. The rating values for the corresponding no-noise image (fig. 7(a)–(d)) were slightly higher for q table 0 (9:1–10:1) and significantly higher for q table 1 (6:1–9:1) and q table 2 (8:1–12:1).

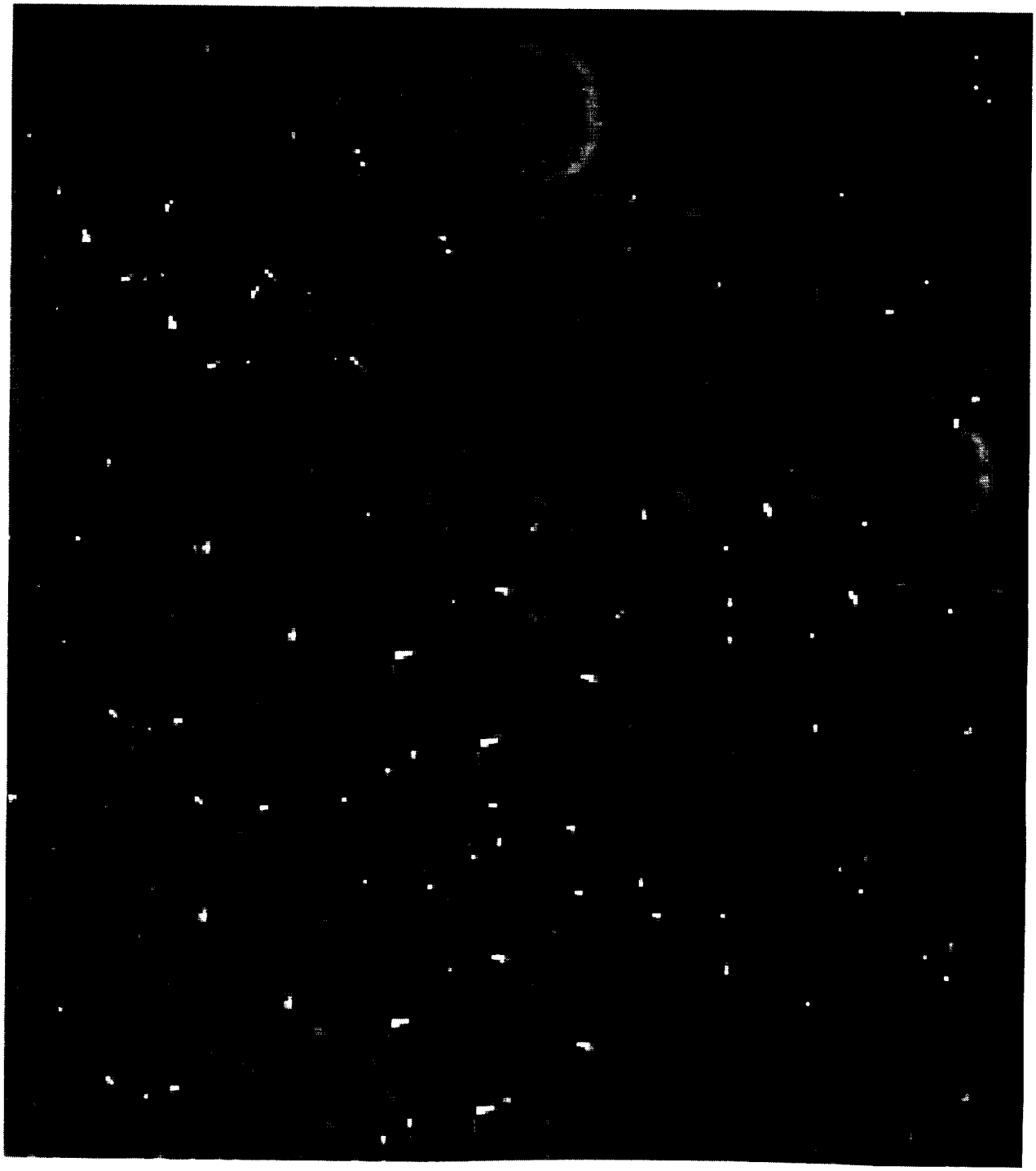

Figure H-4. (a) Image file rq538.g.r (Ganymede) as presented to evaluators.

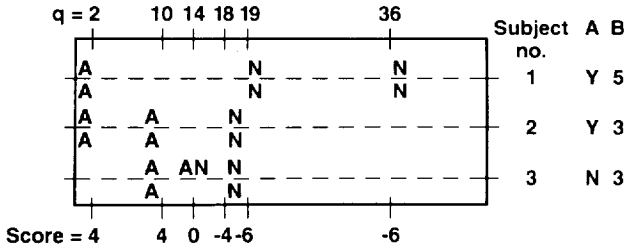

Safe range 10 - 18 Compression ratios 4 - 8
Likely range 10 - 18 Compression ratios 4 - 8

Figure H-4. (b) File rq538.g.r (Ganymede) using q table 0.

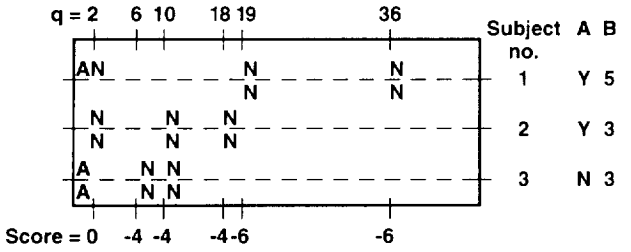

Safe range < 2 Compression ratios < 3
Likely range < 2 Compression ratios < 3

Figure H-4. (c) File rq538.g.r (Ganymede) using q table 1.

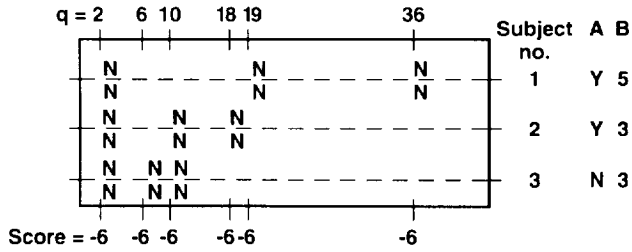

Safe range < 2 Compression ratios < 4
Likely range < 2 Compression ratios < 4

Figure H-4. (d) File rq538.g.r (Ganymede) using q table 2.

Figure H-5(a) is a solid surface image of Io without a limb and with superimposed noise. It was rated by only two evaluators, who were not pleased with the quality of any of the images presented. This fact coupled with the small number of evaluators makes reliability of these results questionable.

Figure H-5. (a) Image file sr7.noise.r (lo) as presented to evaluators.

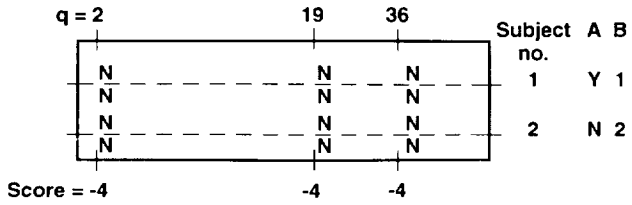

Safe range < 2 Compression ratios = 1
Likely range < 2 Compression ratios = 1

Figure H-5. (b) File sr7.noise.r (lo) using q table 0.

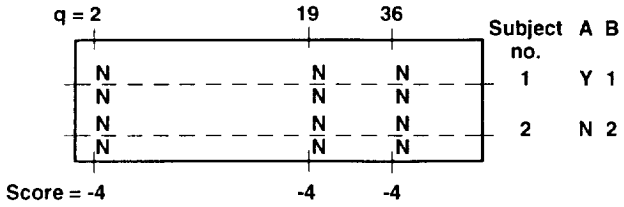

Safe range < 2 Compression ratios < 2
Likely range < 2 Compression ratios < 2

Figure H-5. (c) File sr7.noise.r (lo) using q table 1.

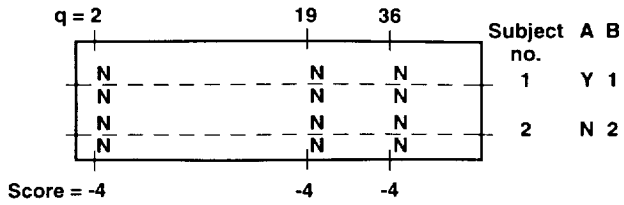

Safe range < 2 Compression ratios < 2
Likely range < 2 Compression ratios < 2

Figure H-5. (d) File sr7.noise.r (lo) using q table 2.

Solid Surface with Terminator– One image without noise (fig. H-6(a)) was studied in this category. Five evaluators rated the image. As shown in figure H-6(a), this image consisted of many bright and dark craters, a plume phenomenon (at the top), a terminator, and approximately 25% (area) sky background. Acceptable ICT compression ratios ranged from 11:1 to 18:1. It is likely that the high proportion of medium- to high-contrast surface details constrained the acceptable compressions to less than 18:1. All three q tables evaluated (fig. H-6(b)–(d)) showed the same regular convergence upon the final acceptable range of compression ratios across the five evaluators (i.e., there was good intra-evaluator stability of rating responses).

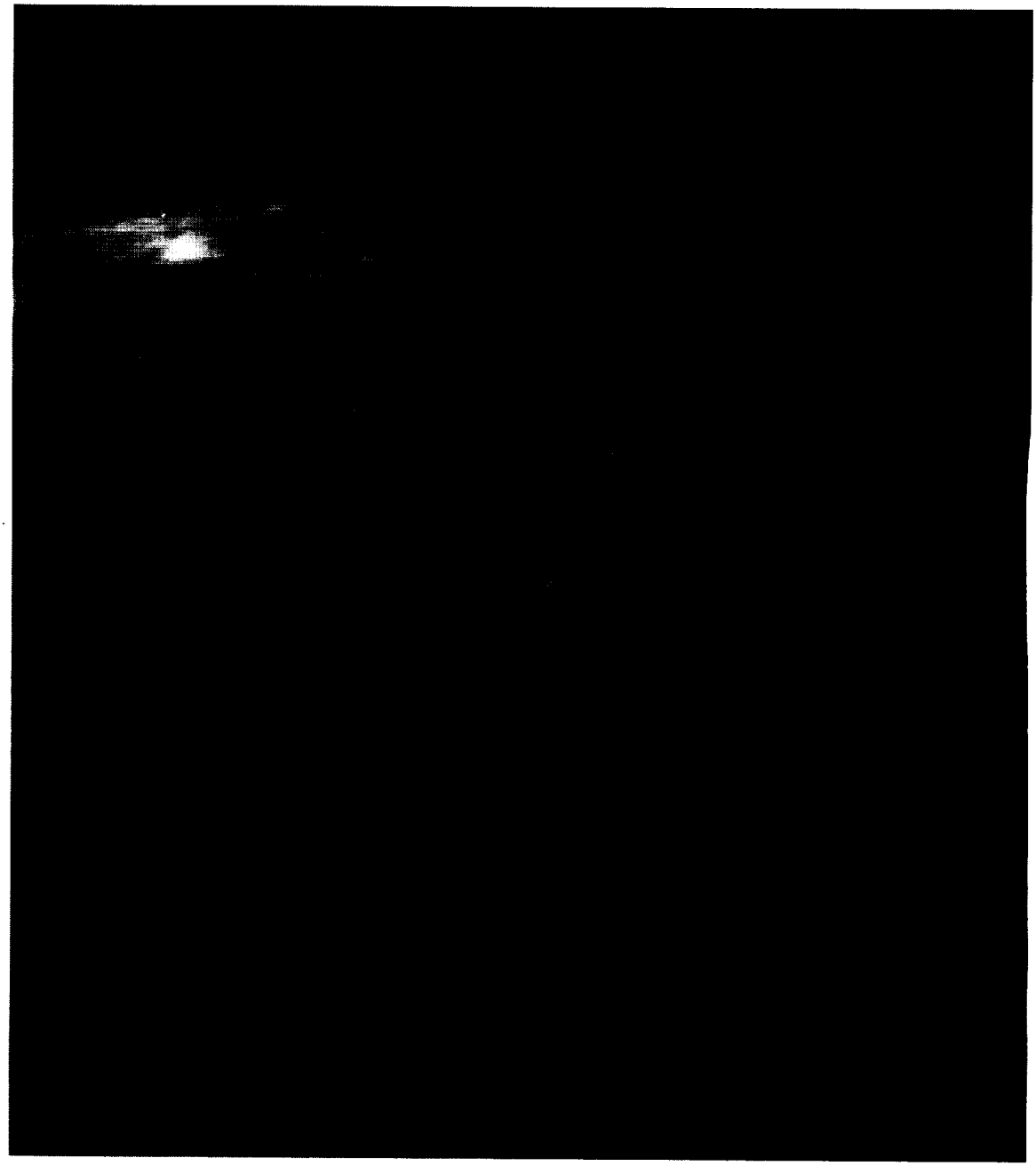

Figure H-6. (a) Image file r.1.r (Callisto) as presented to evaluators.

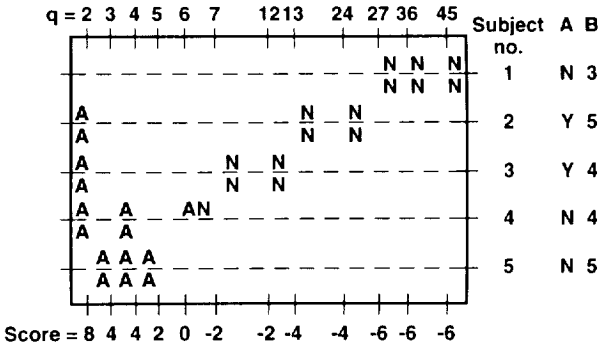

Safe range 5 - 7 **Compression ratios 11 - 17**
Likely range 5 - 7 **Compression ratios 11 - 17**

Figure H-6. (b) File r.1.r (Callisto) using q table 0.

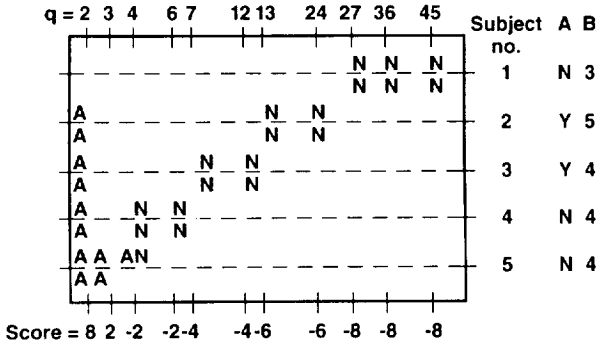

Safe range 3 - 4 **Compression ratios 12 - 15**
Likely range 3 - 4 **Compression ratios 12 - 15**

Figure H-6. (c) File r.1.r (Calisto) using q table 1.

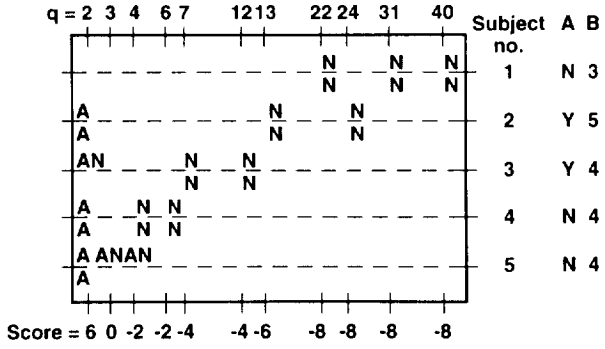

Safe range 2 - 4 **Compression ratios 11 - 18**
Likely range 2 - 4 **Compression ratios 11 - 18**

Figure H-6. (d) File r.1.r (Callisto) using q table 2.

Gaseous surface without limb–As was expected, this type of gaseous surface image (fig. H-7(a)–(d)) yielded relatively high acceptable levels of image compression regardless of which q table was employed. The greatest ICT compression was achieved using q table 3. These data suggest that the three evaluators appeared to use different judgment criteria across these levels. That is, each may have been looking for different phenomena or details and, therefore, each rated the images differently because they did (or did not) see what they were looking for.

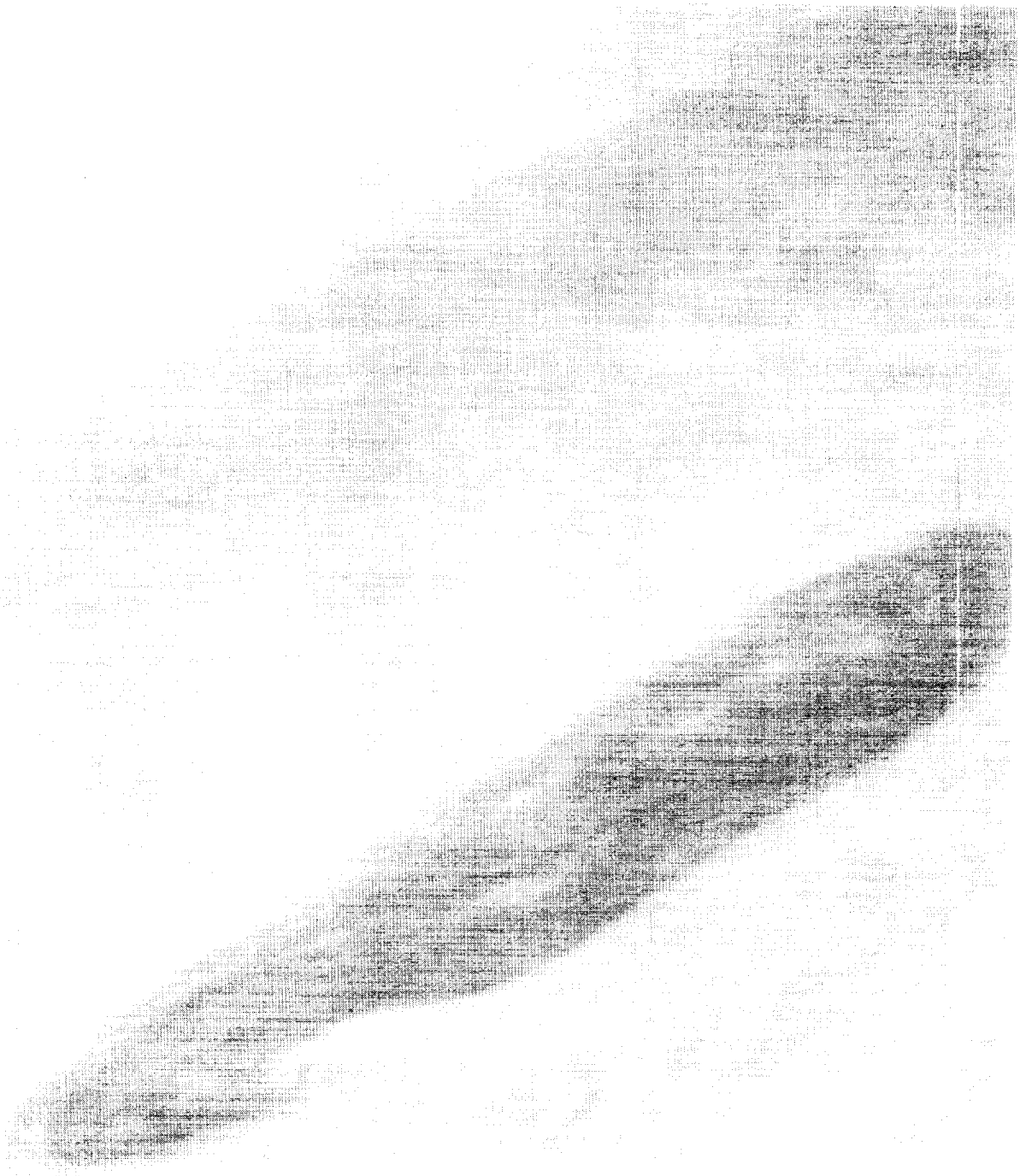

Figure H-7. (a) Image file r.14.r (Jupiter) as presented to evaluators.

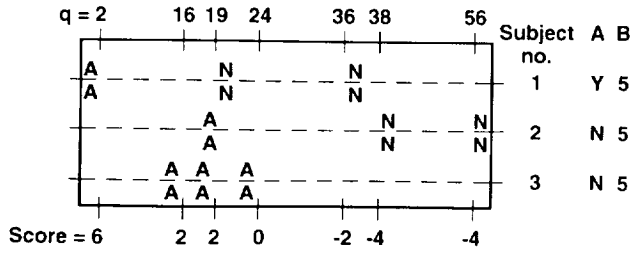

Safe range 24 - 36 Compression ratios 55 - 67
Likely range 24 - 36 Compression ratios 55 - 67

Figure H-7. (b) File r.14.r (Jupiter) using q table 0.

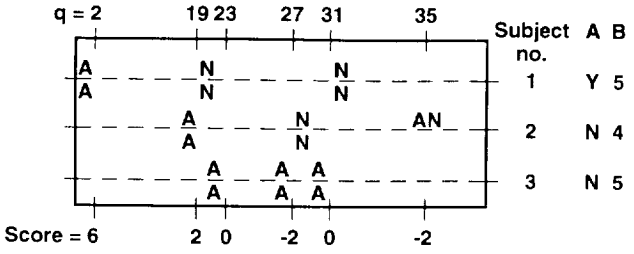

Safe range 19 - 35 Compression ratios 51 - 71
Likely range 19 - 27 Compression ratios 51 - 62

Figure H-7. (c) File r.14.r (Jupiter) using q table 2.

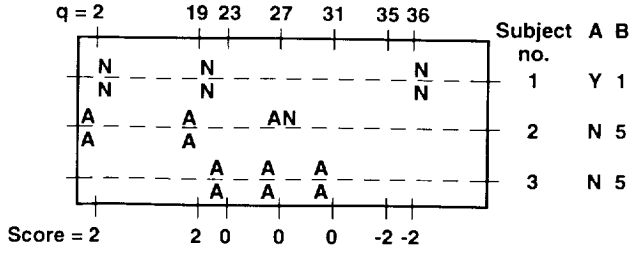

Safe range 19 - 35 Compression ratios 54 - 72
Likely range 19 - 35 Compression ratios 54 - 72

Figure H-7. (d) File r.14.r (Jupiter) using q table 3.

Small bodies (asteroids)– One data file (rq538.gas.r) was available to study this type of image (fig. H-8(a)). The overall image was cropped and three evaluators rated it. Figure H-8(a) consisted of approximately 40% (area) sky background with a relatively high contrast image of cratered surfaces and an irregular terminator. The highest acceptable ICT compression ratios (35:1 to 61:1) were associated with q table 0; q tables 1 and 2 yielded approximately the same level of acceptable compression. As with other images tested, the three evaluators evidenced relatively different evaluation criteria (indicated by their different scores across q levels). Apparently each evaluator was looking for different image details.

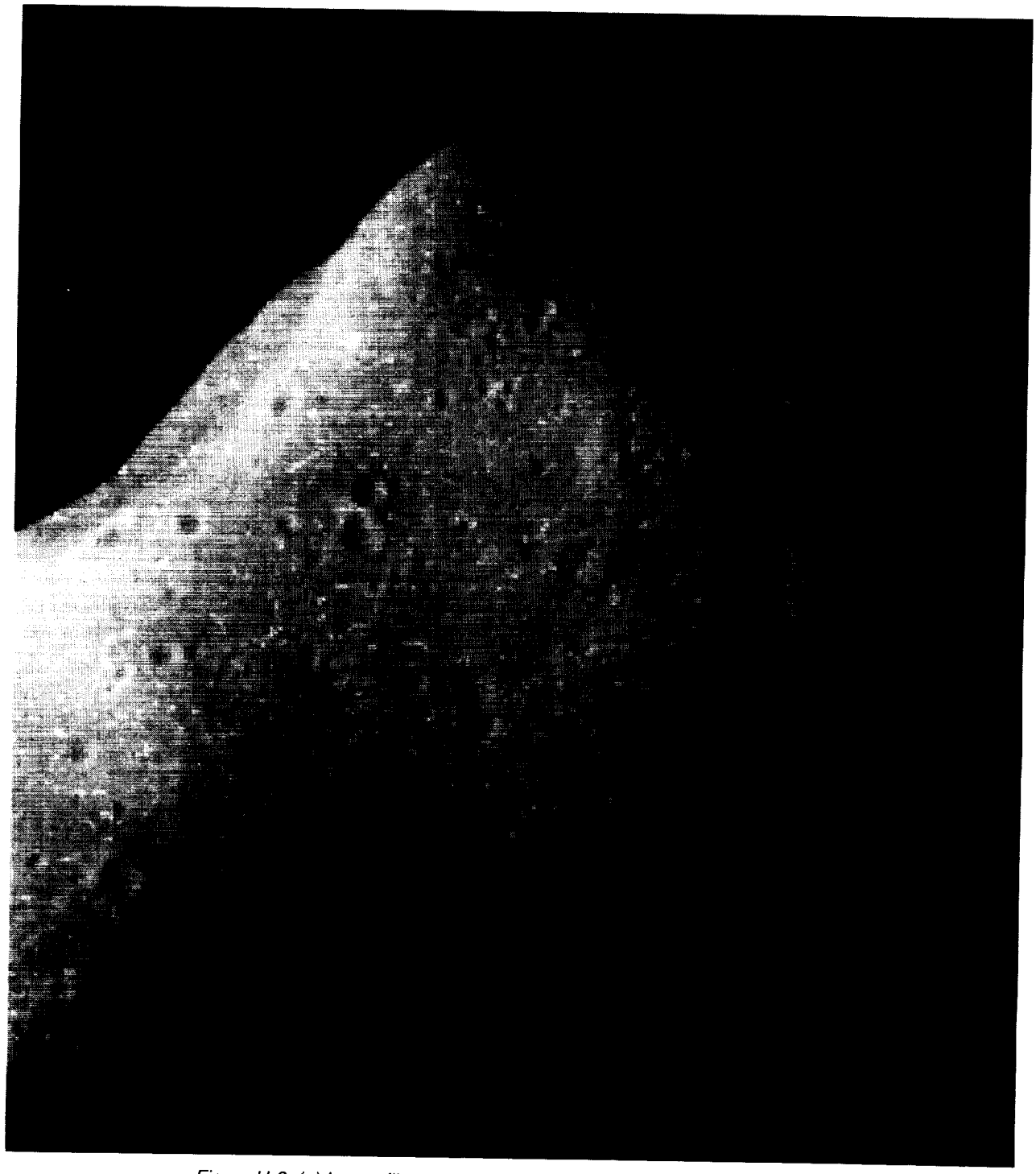

Figure H-8. (a) Image file rq538.gas.r (Gaspra) as presented to evaluators.

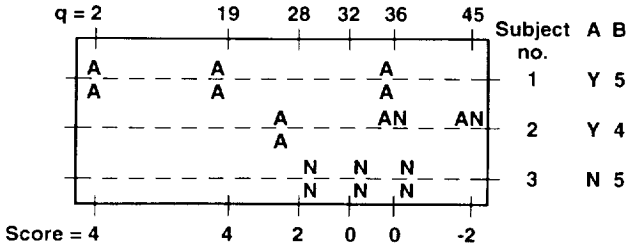

Safe range 28 - 45 Compression ratios 35 - 61
Likely range 28 - 45 Compression ratios 35 - 61

Figure H-8. (b) File rq538.gas.r (Gaspra) using q table 0.

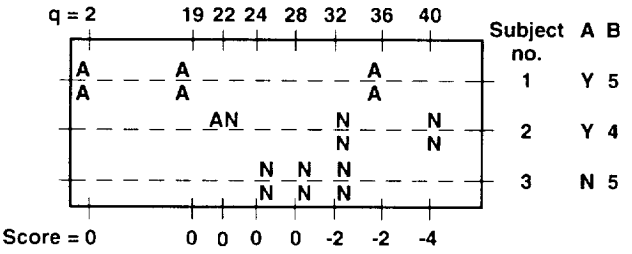

Safe range 22 - 32 Compression ratios 37 - 50
Likely range 22 - 32 Compression ratios 37 - 50

Figure H-8. (c) File rq538.gas.r (Gaspra) using q table 1.

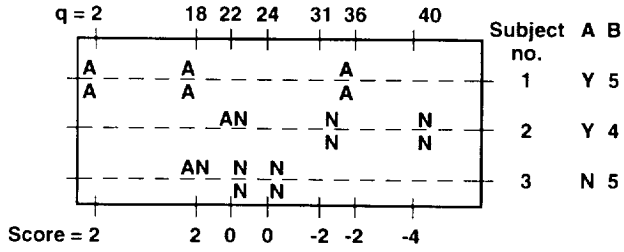

Safe range 18 - 31 Compression ratios 36 - 54
Likely range 18 - 31 Compression ratios 36 - 54

Figure H-8. (d) File rq538.gas.r (Gaspra) using q table 2.

Darkside phenomena/lightning– Three evaluators rated this image (rq538.litn.r), giving the following results. Note that this image (fig H-9(a)) possessed a brightness gradient across its surface that darkened progressively from left to right. It is possible that this gradient could have masked low-contrast phenomena and consequently reduced or eliminated judgments of whether high spatial frequency phenomena were present. The evaluators said they were able to see the bright spots well enough to locate and to count them. Whether or not low-contrast phenomena were actually masked by this luminance gradient could not be assessed during this study. Figure H-9(a) consists of a relatively homogeneous dark field with a number of lighter spots (lightning). This homogeneity accounts for the high levels of acceptable compression achieved (q table 2 yielded ratios of 83:1–88:1).

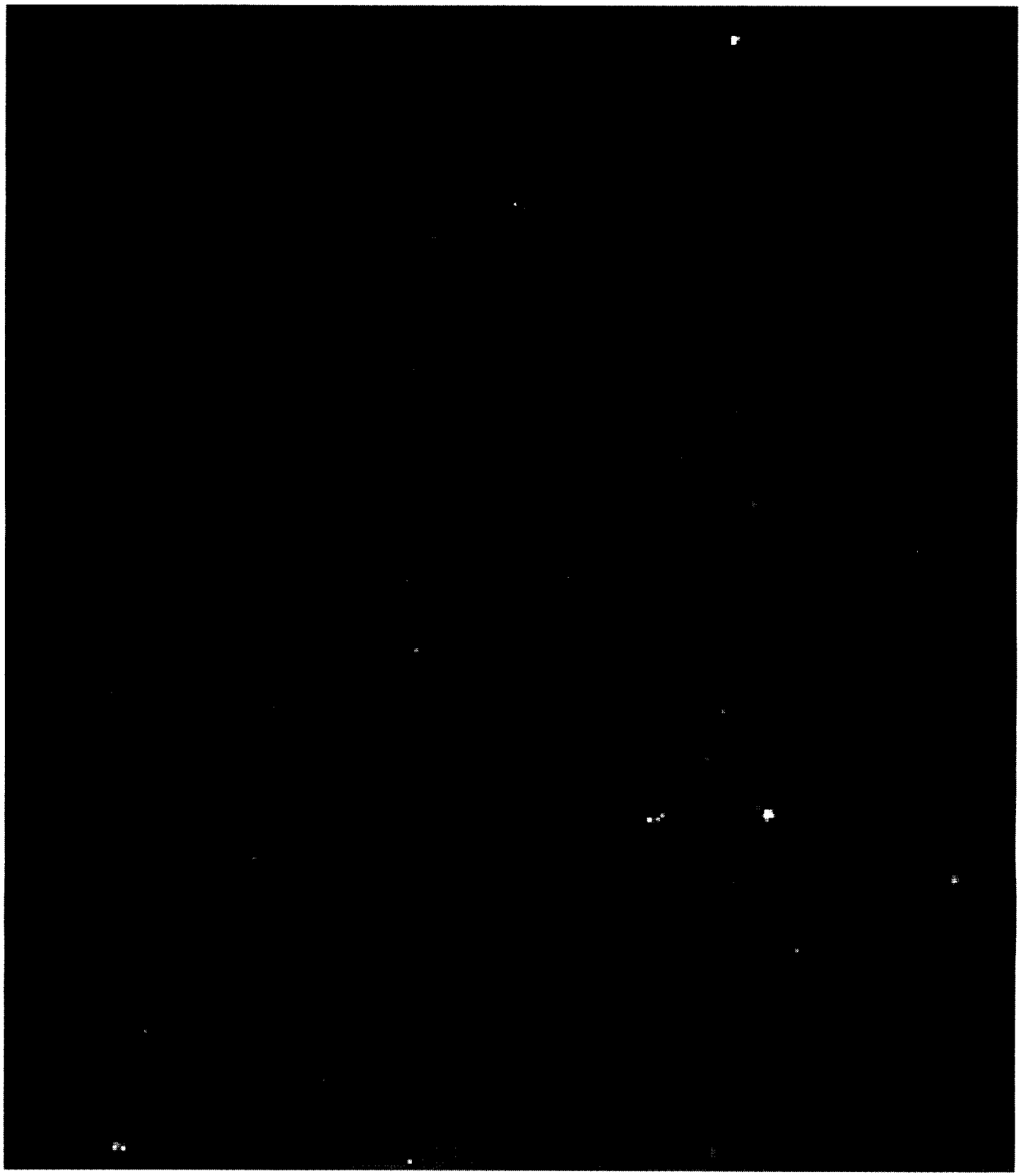

Figure H-9. (a) Image file rq538.litn.r (darkside phenomena) as presented to evaluators.

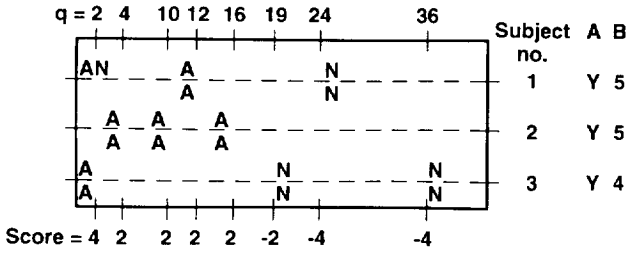

Safe range 16 - 19 Compression ratios 71 - 75
Likely range 16 - 19 Compression ratios 71 - 75

Figure H-9. (b) File rq538.litn.r (darkside phenomena) using q table 0.

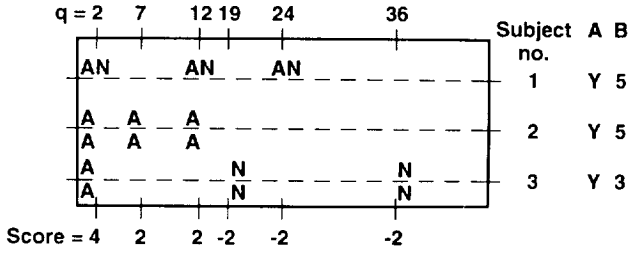

Safe range 12 - 19 Compression ratios 80 - 86
Likely range 12 - 19 Compression ratios 80 - 86

Figure H-9. (c) File rq538.litn.r (darkside phenomena) using q table 1.

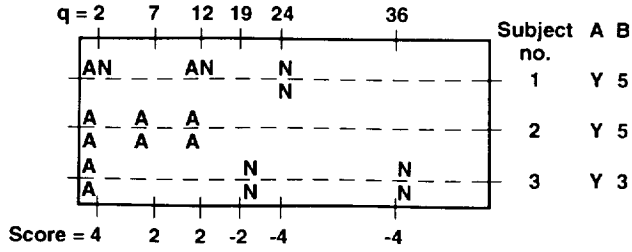

Safe range 12 - 19 Compression ratios 83 - 88
Likely range 12 - 19 Compression ratios 83 - 88

Figure H-9. (d) File rq538.litn.r (darkside phenomena) using q table 2.

Rings– One example (fig. H-10(a)) was available to study this type of high-contrast image (r.11.r). Three evaluators rated it. This high-contrast image possessed both sharply defined curved edges (limb) as well as varying contrast areas (rings). What appeared to be a plume and several point-like bright spots were also present. Maximum acceptable compressions for q tables 2, 1, and 0 were 48:1, 45:1, and 36:1, respectively. Interestingly, all three evaluators rated these levels consistently (almost). This implies that they were looking for the same basic features.

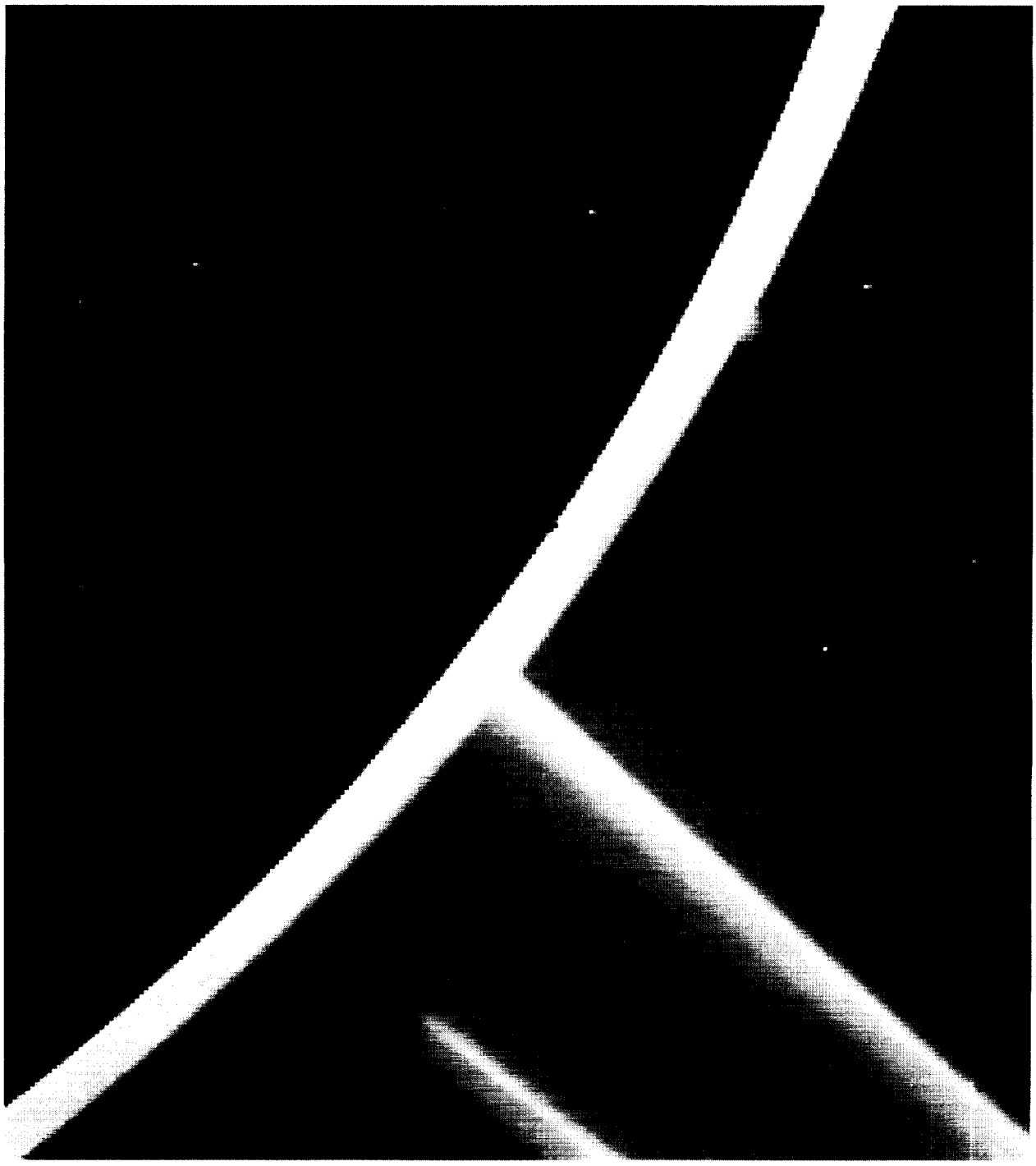

Figure H-10. (a) Image file r.11.r (darkside phenomena) as presented to evaluators.

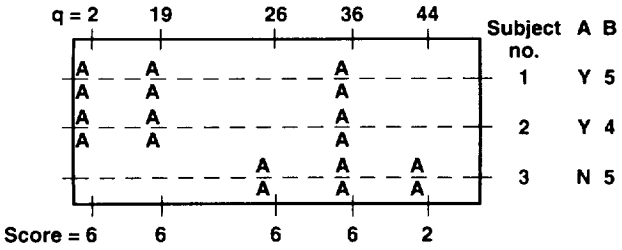

Safe range > 44 **Compression ratios > 36**
Likely range > 44 **Compression ratios > 36**

Figure H-10. (b) File r.11.r (darkside phenomena) using q table 0.

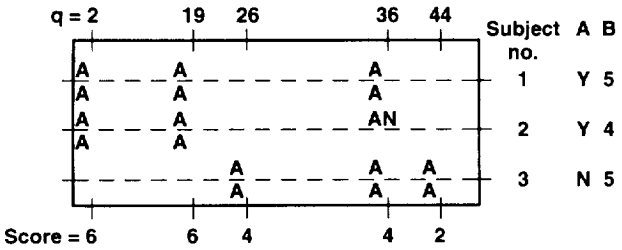

Safe range > 44 **Compression ratios > 45**
Likely range > 44 **Compression ratios > 45**

Figure H-10. (c) File r.11.r (darkside phenomena) using q table 1.

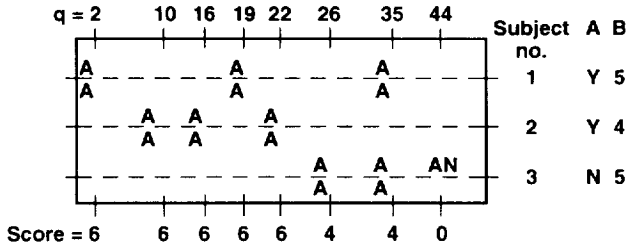

Safe range > 44 **Compression ratios > 48**
Likely range > 44 **Compression ratios > 48**

Figure H-10. (d) File r.11.r (darkside phenomena) using q table 2.

I. Correspondence from Dr. Kar-Ming Cheung, Jet Propulsion Laboratory

National Optical Astronomy Observatories

950 N. Cherry Ave.
P.O. Box 26732 Tucson, Arizona 85726-6732
(602) 327-5511 FAX: (602) 325-9360
Telex 1561401 Aura Ut
Internet: noao @ noao. edu

Kitt Peak National Observatory • Cerro Tololo Inter-American Observatory • National Solar Observatory

Dr Kar-Ming Cheung
MS 238-420
JPL
4800 Oak Grove Drive
Pasadena CA 91109-8099

August 10, 1993

Dear Kar-Ming,

I have just received a copy of the Preliminary Report of the "Image Evaluation Experiment' done at Ames R.C. on July 22, 1993, and would like to share with you my thoughts about it.

1. The three primary conclusions:

- Acceptable compression ratios vary widely with the image;
- Noisy images detract greatly from image acceptability and acceptable compression ratios;
- Atmospheric images of Jupiter seem to have higher acceptable compression ration of 4 to 5 times that of some satellite images.

are qualitatively in concert with the experience of the team from its own studies of the effects of compression.

2. The numerical Compression Ratios in Table 2 labeled "Acceptable" have the same trends as have been derived from the teams own studies, i.e.:

- Atmospheric images can take more compression that satellite images;
- Radiation noise in the images rapidly reduces the acceptable level of compression.

However, the numerical values are, in the cases without noise, generally much higher in the Ames experiment than allowed by our own experience. This is, in my opinion, quite clearly due to the fact that the criteria in the Ames experiment were basically related to a simple "visual acceptance" of an image and not the reflection of the measurement of some quantitative property of the image. For atmospheric pictures with little noise, the teams

Operated by the Association of Universities for Research in Astronomy, Inc. (AURA) under cooperative agreement with the National Science Foundation

experience seems to be point at compression ratios between 20:1 and 30:1, i.e. about 60% of the Ames numbers. For satellites, were Galileo/SSI will produce scenes of much higher complexity (10 to 100 times higher resolution) than did Voyager, the team's experience is heading for an upper limit to the acceptable compression ratio of 10:1 in the absence of noise, and 2:1 to 3:1 when noise is present at the predicted levels. My preliminary assessment of the team's current experience is, in the case of satellites, roughly the same as the results shown for Calisto and Ganymede in Table 2 of the Ames study report.

3. Finally, I find it interesting that the Ames study does find some, if only a modest amount, dependence on the Q-matrix that was used.....with different matrices favored for different targets. Clearly we will need everything that could possibly be to our advantage for a successful imaging experiment on the Galileo orbital mission, and so the search for an optimized set of Q-matrices continues to be of considerable importance. Individuals on the team are currently pursuing such a search in areas of interest to them.

The Ames experiment was an interesting step and yielded results that make sense in terms of the trends that were revealed. However, as a quantitative measure of acceptable compression ratios the quantitative results of the study do not, in my opinion, fare so well.

To reduce the chance that the numbers of Table 2 will not be misinterpreted by others, I would appreciate it if you would always be sure to attach a copy of this letter to the report whenever you share it with your colleagues.

With best regards,

Michael J.S. Belton
SSI Team Leader.

cc. Galileo/SSI Imaging Team

REPORT DOCUMENTATION PAGE

Form Approved
OMB No. 0704-0188

Public reporting burden for this collection of information is estimated to average 1 hour per response, including the time for reviewing instructions, searching existing data sources, gathering and maintaining the data needed, and completing and reviewing the collection of information. Send comments regarding this burden estimate or any other aspect of this collection of information, including suggestions for reducing this burden, to Washington Headquarters Services, Directorate for information Operations and Reports, 1215 Jefferson Davis Highway, Suite 1204, Arlington, VA 22202-4302, and to the Office of Management and Budget, Paperwork Reduction Project (0704-0188), Washington, DC 20503.

1. AGENCY USE ONLY *(Leave blank)*	2. REPORT DATE	3. REPORT TYPE AND DATES COVERED
	July 1994	Technical Paper

4. TITLE AND SUBTITLE
Subjective Evaluations of Integer Cosine Transform Compressed Galileo Solid State Imagery

5. FUNDING NUMBERS
476-14-03

6. AUTHOR(S)
Richard F. Haines,* Yaron Gold,* Terry Grant, and Sherry Chuang

7. PERFORMING ORGANIZATION NAME(S) AND ADDRESS(ES)
Ames Research Center
Moffett Field, CA 94035-1000

8. PERFORMING ORGANIZATION REPORT NUMBER
A-94068

9. SPONSORING/MONITORING AGENCY NAME(S) AND ADDRESS(ES)
National Aeronautics and Space Administration
Washington, DC 20546-0001

10. SPONSORING/MONITORING AGENCY REPORT NUMBER
NASA TP-3482

11. SUPPLEMENTARY NOTES
Point of Contact: Terry Grant, Ames Research Center, MS 269-4, Moffett Field, CA 94035-1000; (415) 604-4200
*RECOM Technologies, Inc., Ames Research Center, -Moffett Field, CA 95035-1000

12a. DISTRIBUTION/AVAILABILITY STATEMENT
Unclassified — Unlimited
Subject Categories 89, 53

Available from the NASA Center for AeroSpace Information,
800 Elkridge Landing Road, Linthicum Heights, MD 21090; (301) 621-0390

12b. DISTRIBUTION CODE

13. ABSTRACT *(Maximum 200 words)*

This paper describes a study conducted for the Jet Propulsion Laboratory, Pasadena, California, using 15 evaluators from 12 institutions involved in the Galileo Solid State Imaging (SSI) experiment. The objective of the study was to determine the impact of integer cosine transform (ICT) compression using specially formulated quantization (q) tables and compression ratios on acceptability of the 800 × 800 × 8 monochromatic astronomical images as evaluated visually by Galileo SSI mission scientists. Fourteen different images in seven image groups were evaluated. Each evaluator viewed two versions of the same image side by side on a high-resolution monitor; each was compressed using a different q level. First the evaluators selected the image with the highest overall quality to support them in their visual evaluations of image content. Next they rated each image using a scale from one to five indicating its judged degree of usefulness. Up to four preselected types of images with and without noise were presented to each evaluator.

14. SUBJECT TERMS	15. NUMBER OF PAGES
Image compression, Galileo Project, Integer cosine transform, ICT, Subjective evaluations	70
	16. PRICE CODE A04

17. SECURITY CLASSIFICATION OF REPORT	18. SECURITY CLASSIFICATION OF THIS PAGE	19. SECURITY CLASSIFICATION OF ABSTRACT	20. LIMITATION OF ABSTRACT
Unclassified	Unclassified		